CANCER

Preneoplastic somatic mutations including *MYD88*[L265P] in lymphoplasmacytic lymphoma

Sara Rodriguez[1]†, Jon Celay[1]†, Ibai Goicoechea[1]†, Cristina Jimenez[2]†, Cirino Botta[3], Maria-José Garcia-Barchino[1], Juan-Jose Garces[1], Marta Larrayoz[1], Susana Santos[4], Diego Alignani[1], Amaia Vilas-Zornoza[1], Cristina Perez[1], Sonia Garate[1], Sarai Sarvide[1], Aitziber Lopez[1], Hans-Christian Reinhardt[5], Yolanda R. Carrasco[6], Isidro Sanchez-Garcia[7], Maria-Jose Larrayoz[1], Maria-Jose Calasanz[1], Carlos Panizo[1], Felipe Prosper[1], Jose-Maria Lamo-Espinosa[1], Marina Motta[8], Alessandra Tucci[8], Antonio Sacco[9], Massimo Gentile[10], Sara Duarte[4], Helena Vitoria[11], Catarina Geraldes[4], Artur Paiva[4], Noemi Puig[2], Ramon Garcia-Sanz[2], Aldo M. Roccaro[9], Gema Fuerte[12], Jesus F. San Miguel[1], Jose-Angel Martinez-Climent[1]*‡, Bruno Paiva[1]*‡

Normal cell counterparts of solid and myeloid tumors accumulate mutations years before disease onset; whether this occurs in B lymphocytes before lymphoma remains uncertain. We sequenced multiple stages of the B lineage in elderly individuals and patients with lymphoplasmacytic lymphoma, a singular disease for studying lymphomagenesis because of the high prevalence of mutated *MYD88*. We observed similar accumulation of random mutations in B lineages from both cohorts and unexpectedly found *MYD88*[L265P] in normal precursor and mature B lymphocytes from patients with lymphoma. We uncovered genetic and transcriptional pathways driving malignant transformation and leveraged these to model lymphoplasmacytic lymphoma in mice, based on mutated *MYD88* in B cell precursors and *BCL2* overexpression. Thus, *MYD88*[L265P] is a preneoplastic event, which challenges the current understanding of lymphomagenesis and may have implications for early detection of B cell lymphomas.

INTRODUCTION

The identity, number, and order of events that initiate and drive tumorigenesis from normal cells remain largely unknown (*1*). It is only recently that sequencing studies of small biopsies have shown that normal cell counterparts of various solid tumors accumulate several mutations years before disease onset (*2–5*). Although some of these mutations show clear signs of positive selection and hit well-known cancer genes, they do not immediately lead to cancer (*1*). Hence, the emerging landscapes of somatic mutations in normal bladder (*5*), colon (*6*, *7*), endometrium (*8*, *9*), liver (*10*, *11*), esophagus (*4*, *12*, *13*), and skin (*14*) cells are challenging classical models of cancer development.

The presence of clonal hematopoiesis in the elderly, and its association with an increased risk of developing myeloid malignancies (*15*, *16*), has changed the way aging is viewed in hematology (*17*).

While clonal hematopoiesis reflects the differentiation of mutated CD34-positive hematopoietic stem/progenitor cells (HPCs) into multiple lineages circulating in peripheral blood, de novo gene mutations can affect individual compartments such as B lymphocytes (*18–20*). Mutations in the B cell lineage also increase significantly with age (*19*), are present both inside and outside the immunoglobulin (Ig) loci (*18*), and are detectable in genes commonly altered in B cell disorders (*19*, *20*). These findings suggest that there is a preneoplastic stage in human lymphomagenesis; however, the genetic events that occur in normal cells before onset of lymphoma remain largely unknown (*21–24*).

The L265P mutation in the myeloid differentiation primary response 88 (MYD88) protein mimics a constitutive Toll-like receptor activation and potentiates B cell receptor (BCR)–mediated nuclear factor κB (NF-κB) signaling, promoting lymphocyte proliferation and survival (*25*, *26*). *MYD88*[L265P] is commonly detected in patients with IgM lymphoplasmacytic lymphoma or Waldenström's macroglobulinemia (LPL/WM) (*27*). However, it is also present in some patients with diffuse large B cell lymphoma (DLBCL), marginal zone lymphoma, and chronic lymphocytic leukemia (CLL) (*28*). Thus, individuals with *MYD88*[L265P] may go on to develop various lymphoma types other than LPL/WM.

The disease characteristics of LPL/WM mean that it provides a singular model for studying lymphomagenesis: (i) There is a very high prevalence of *MYD88*[L265P] in patients with LPL/WM, providing a genetic marker of the disease; (ii) LPL/WM displays bone marrow (BM) infiltration of mutated B lymphocytes and plasma cells (PCs) (*29*), allowing for the characterization of intratumor diversity; and (iii) LPL/WM is preceded by the premalignant condition IgM monoclonal gammopathy of undetermined significance (MGUS), enabling the observation of clonal evolution before the development of the full-blown disease. Notably, it has previously been shown that *MYD88*[L265P] is detectable in most cases of IgM MGUS (*30*, *31*).

[1]Clinica Universidad de Navarra, Centro de Investigacion Medica Aplicada (CIMA), Instituto de Investigacion Sanitaria de Navarra (IDISNA), CIBER-ONC, Pamplona, Spain. [2]Hospital Universitario de Salamanca, Instituto de Investigacion Biomedica de Salamanca (IBSAL), Centro de Investigación del Cancer (IBMCC-USAL, CSIC), CIBER-ONC, Salamanca, Spain. [3]Department of Health Promotion, Mother and Child Care, Internal Medicine and Medical Specialties, University of Palermo, Palermo, Italy. [4]Centro Hospitalar e Universitario de Coimbra, Coimbra, Portugal. [5]Department of Hematology and Stem Cell Transplantation, West German Cancer Center, DKTK Partner Site Essen, Center for Molecular Biotechnology, University Hospital Essen, Hufelandstr. 55, 45147, Essen, Germany. [6]Department of Immunology and Oncology, Centro Nacional de Biotecnología (CNB)–CSIC, Madrid, Spain. [7]Experimental Therapeutics and Translational Oncology Program, Instituto de Biología Molecular y Celular del Cáncer, CSIC/Universidad de Salamanca and Institute of Biomedical Research of Salamanca (IBSAL), Salamanca, Spain. [8]Department of Hematology, ASST Spedali Civili di Brescia, Brescia, Italy. [9]Clinical Research Development and Phase I Unit, ASST Spedali Civili di Brescia, Brescia, Italy. [10]Department of Oncohematology, "Annunziata" Hospital, Cosenza, Italy. [11]Hospital de S. Teotónio, Viseu, Portugal. [12]Mission Bio, San Francisco, CA, USA.
*Corresponding author. Email: jamcliment@unav.es (J.-A.M.-C.); bpaiva@unav.es (B.P.)
†These authors contributed equally to this work as co–first authors.
‡These authors contributed equally to this work as co–senior authors.

However, even after a median follow-up of 34 years, approximately 84% of individuals with IgM MGUS do not progress to LPL/WM or other lymphoma (*32*). Therefore, many patients with $MYD88^{L265P}$ do not develop a B cell malignancy.

We hypothesized that progression from $MYD88^{L265P}$ to malignant lymphoma may be fundamentally driven by both the cellular origin of the $MYD88^{L265P}$ mutation and the emergence of cooperating genetic alterations; this idea has not been investigated previously. Therefore, we sought to identify the stage during hematopoietic development at which $MYD88^{L265P}$ and other genetic alterations arise in elderly individuals without cancer and in patients with LPL/WM.

RESULTS

Mutations during B cell lymphopoiesis in elderly individuals and patients with LPL/WM

We used fluorescence-activated cell sorting (FACS) to isolate CD34-positive HPCs, B cell precursors, and mature B lymphocytes from BM aspirates of five elderly individuals aged between 67 and 85 years (ID #20 to #24; table S1) and 10 newly diagnosed patients with LPL/WM aged between 54 and 83 years (ID #1 to #10; table S1) (Fig. 1A). The use of high-purity FACS based on multidimensional monoclonal antibody (mAb) combinations and guided by patient-specific tumor phenotypes (*33*) enabled, for patients with LPL/WM, simultaneous isolation of tumor B cells and PCs, in addition to the three normal cell types identified above (fig. S1 and table S1). Although T/natural killer (NK) lymphocytes are an imperfect control in these analyses, they were used nonetheless to exclude germline variants. We compared the somatic mutation burden at the different stages of B cell lymphopoiesis in both cohorts by whole exome sequencing (WES) with molecular barcoding.

We found an average of 138, 206, and 189 somatic mutations in CD34-positive HPCs, B cell precursors, and mature B lymphocytes, respectively, from elderly individuals, and similar averages of 141 ($P = 0.86$), 142 ($P = 0.99$), and 203 ($P = 0.32$) in the respective cells from patients with LPL/WM (Fig. 1B). The single-base substitution 4 (SBS4; related to tobacco smoking) and SBS5 (of unknown etiology, but possibly clock-like) mutational signatures were identified upon analyzing all somatic mutations observed in the entire cohort of individuals and cell types (fig. S2A).

Of the 1969 and 3032 somatic mutations detected in maturation subsets from elderly individuals and patients (table S2), respectively, only 399 (20%) and 811 (27%) were shared by two or all three cell subsets (Fig. 1C). These results suggest that somatic mutations are predominantly due to ongoing random mutations occurring over the course of B cell lymphopoiesis in both elderly individuals (1570 of 1969 somatic mutations; 80%) and patients with LPL/WM (2221 of 3032; 73%), rather than mutated CD34-positive HPCs or B cell precursors positively differentiating into mature B lymphocytes. Accordingly, the distribution of nonsense and missense variants, insertions and deletions, was similar between shared and private mutations (fig. S2B).

Somatic mutations were spread throughout the exome. Although the chromosome arm unit of measure has poor resolution, there were no significant differences in the number of mutations between elderly individuals and patients with LPL/WM per chromosome arm (Fig. 1D). In elderly individuals and patients with LPL/WM, respectively, only 1 of 1969 (0.05%) and 4 of 3032 (0.13%) somatic

mutations were observed in the constant region of Ig loci. Variable regions where somatic hypermutations are expected were not analyzed because of limitations of the methodology.

Overall, among elderly individuals and patients with LPL/WM, we detected 15 recurrent somatic mutations occurring in one or more of the different stages of B cell lymphopoiesis. Of these, mutations in the $MYD88$ gene were exclusively observed in patients with LPL/WM (table S3). $MYD88^{L265P}$ was undetectable in the B cell lymphopoiesis of six additional elderly individuals, using allele-specific oligonucleotide polymerase chain reaction (ASO-PCR).

$MYD88^{L265P}$ in normal B cell precursors and B lymphocytes from patients with LPL/WM

$MYD88^{L265P}$ was not only detected by WES in tumor B cells and PCs from all patients with LPL/WM but was also seen in phenotypically normal B cell precursors from one of nine patients and mature B lymphocytes from four of six patients (Fig. 2A). Mutations in $MYD88$ were never detected in T/NK lymphocytes. To analyze for possible contamination arising during FACS, we used the high-throughput capacity of WES to investigate whether other clonal mutations present in $MYD88^{L265P}$ tumor B cells and PCs were also seen in $MYD88^{L265P}$ phenotypically normal cells, which would indicate co-isolation of contaminating tumor cells. Specifically, we investigated the presence, in normal cell types, of somatic mutations with high clonal cell fraction (CCF) (i.e., >0.7) in tumor B cells (table S4). We found that 9 of 17 (53%) and 36 of 66 (55%) of these mutations were undetectable in B cell precursors and mature B lymphocytes, respectively. While these findings do not exclude the possible contamination during FACS, they do preclude this being the reason for our observation of $MYD88^{L265P}$ in patients' phenotypically normal cells.

To confirm the presence of $MYD88^{L265P}$ in these phenotypically normal cells, we used two PCR methods [ASO-PCR and droplet digital PCR (dd-PCR)] and single-cell DNA sequencing (scDNA-seq) of $MYD88$ plus oligo-coupled mAb targeting CD10, CD19, CD20, CD27, CD34, and CD38 for unbiased cell clustering. With the higher sensitivity of ASO-PCR and dd-PCR [limit of detection, 10^{-3} to 10^{-6} (*31*, *34*)] compared to WES (average sequencing depth of 112×), we detected $MYD88^{L265P}$ in more patients' B cell precursors ($n = 6$ of 8) and normal B lymphocytes ($n = 6$ of 6), as well as in CD34-positive HPCs from one patient (Fig. 2A). The prevalence of $MYD88^{L265P}$ in CD34-positive HPCs and B cell precursors was further evaluated using ASO-PCR or dd-PCR in seven additional patients with LPL/WM; the mutation was observed in B cell precursors from all cases, but not in CD34-positive HPCs (table S5). High-sensitivity scDNA-seq showed the systematic presence of $MYD88^{L265P}$ in CD34-positive HPCs, B cell precursors, and normal and tumor mature B lymphocytes from four patients with LPL/WM analyzed with this methodology (ID #16 to #19; table S1) (Fig. 2B).

On WES, the allele frequency (AF) of $MYD88^{L265P}$ in normal B cell precursors (median, 0.05; range, 0.02 to 0.16) and mature B lymphocytes (median, 0.11; range, 0.06 to 0.12) was significantly lower than the CCF found in tumor B cells (median, 0.90; range, 0.62 to 1.0; $P = 0.0007$) and PCs (median, 0.72; range, 0.08 to 1.0; $P = 0.0018$). On the basis of dd-PCR, $MYD88^{L265P}$ AF was similarly very low in normal cell types (median, 0.08%; Table 1). scDNA-seq revealed progressively higher percentages of $MYD88^{L265P}$ in CD34-positive HPCs (12%), B cell precursors (33%), and normal and tumor mature B lymphocytes (53%) (Fig. 2B).

Fig. 1. Mutations during B cell lymphopoiesis in elderly individuals and patients with LPL/WM. (**A**) Schematic of workflow, including subject disposition, BM cell types isolated by FACS, and methodology used for WES. (**B**) Average numbers and range of somatic mutations in CD34-positive HPCs, B cell precursors, and mature B lymphocytes from elderly individuals (*N* = 5) and patients with LPL/WM (*N* = 10). Colors indicate types of mutations. (**C**) Absolute numbers and percentages of shared mutations across the different stages of B cell lymphopoiesis in elderly individuals and patients with LPL/WM. (**D**) Rainfall plot of somatic mutations detected in cells from the different stages of B cell lymphopoiesis from elderly individuals and patients with LPL/WM. Mutations are ordered from left to right along the *x* axis from the first variant on the short arm of chromosome 1 (chr1) to the last variant on the long arm of chromosome Y. The vertical axis shows the distance between each mutation and the previous one on a logarithmic scale. Density of mutations, based on the number and intermutation distances, is shown across the top of each rainfall plot.
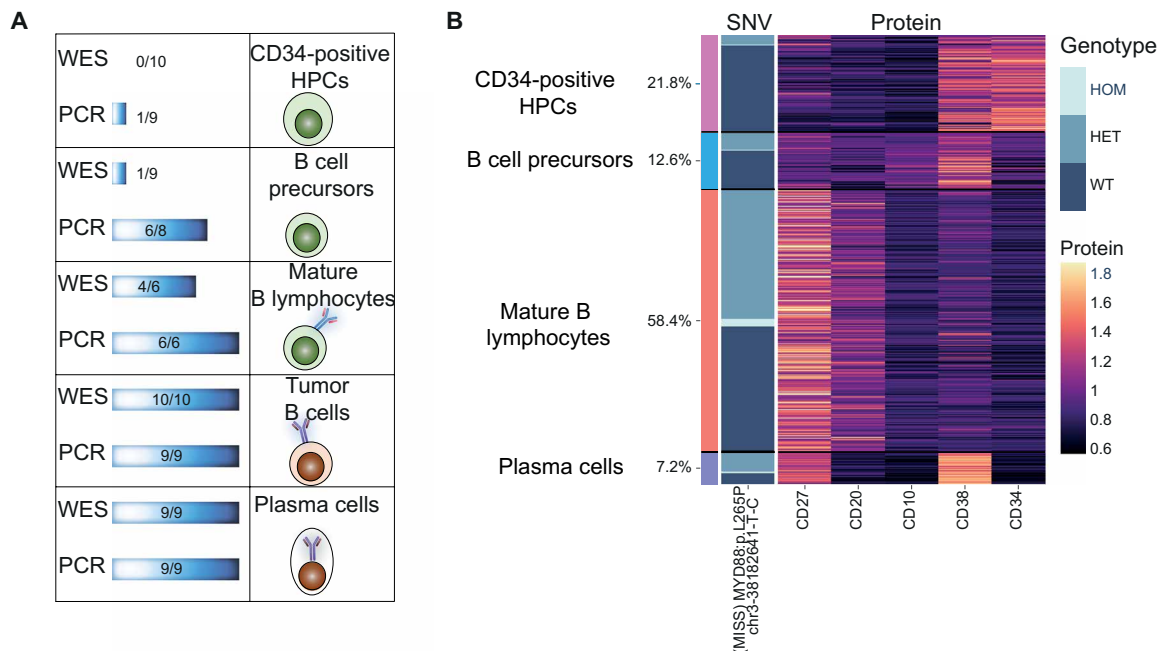
Fig. 2. *MYD88*[L265P] in normal B cell precursors and B lymphocytes from patients with LPL/WM. (**A**) Frequency of *MYD88*[L265P] mutation, as assessed by WES and by ASO-PCR or droplet digital PCR (dd-PCR), in CD34-positive HPCs, B cell precursors, mature B lymphocytes, tumor B cells, and PCs from patients with LPL/WM. (**B**) Presence of wild-type (WT) versus heterozygous (HET) or homozygous (HOM) *MYD88*[L265P] in 10,891 CD34-positive HPCs, B cell precursors, and mature B lymphocytes isolated by FACS from four patients with LPL/WM and stained with oligo-coupled mAbs targeting CD10, CD19, CD20, CD27, CD34, and CD38. Color scale indicates the intensity of antigen expression.

Genetic evolution during lymphomagenesis: Shared and private somatic mutations in normal cells and tumor cells from patients with LPL/WM

Our dataset of somatic mutations in normal and tumor cells from patients with LPL/WM provided an opportunity to identify patterns of genetic evolution during lymphomagenesis. We identified an average of 156 (range, 25 to 291) shared somatic mutations between any normal cell type and tumor cells (Fig. 3A), including averages of 79 (range, 12 to 132), 95 (range, 21 to 124), and 95 (range, 26 to 197) shared somatic mutations between tumor B cells and CD34-positive HPCs, B cell precursors, and mature B lymphocytes, respectively. We further identified an average of nine mutations (range, 0 to 37) that were shared across all cell types, from CD34-positive HPCs to tumor B cells and PCs (Fig. 3B and table S6).

Conversely, an average of 44 mutations [range, 31 to 175; median CCF, 0.18 (range, 0.01 to 1.0)] were unique to tumor B cells (Fig. 3B). *CXCR4*, *IGLL5*, and *NADH3* were the only recurrently mutated genes associated with progression to LPL/WM; these mutations were not seen in normal cells, even those with *MYD88*[L265P] (table S4). Other pan-cancer genes such as *TP53* and *DICER1* were exclusively mutated in tumor B cells from individual patients (table S4). Furthermore, we identified eight copy number abnormalities (CNAs) in tumor cells (table S7), none of which were found in normal cells. These results reveal the individual patient-level genetic alterations that drove progression from preneoplastic mutations in B cell lymphopoiesis to LPL/WM.

Intratumor heterogeneity in LPL/WM

Neoplastic transformation of premalignant IgM MGUS to LPL/WM is characterized by a significant increase in IgM secreted by clonal PCs, which differentiate from tumor B cells (*29*). We compared the genomic landscapes of tumor B cells and PCs to investigate whether clonal evolution occurred during lymphoplasmacytic differentiation. We found only 724 of 2395 (30%) mutations and four of eight (50%) CNAs shared between these two clonal stages (Fig. 3A); tumor B cells had 818 of 2395 (34%) mutations and four of eight (50%) CNAs that were undetectable in PCs, whereas PCs had 853 of 2395 (36%) private mutations but no private CNAs. These results were confirmed using scDNA-seq with amplicons covering multiple regions in regulatory genes of chromosome 6q (fig. S3), which is commonly deleted in patients with LPL/WM (*27*). Collectively, these findings show that not all tumor B cells differentiate into PCs, particularly those with CNAs such as del(6q), which may potentially block B cell differentiation through loss of *PRDM1* (*35*). The data also support the concept of continuous genetic evolution upon differentiation, with tumor B cells and PCs harboring an average of 44 and 59 private somatic mutations, respectively (Fig. 3B).

Malignant transformation of IgM MGUS to LPL/WM

All clonally related B cells must share the same BCR gene rearrangement. We performed single-cell RNA and BCR sequencing (scRNA/BCR-seq) in a total of 42,204 B cells and PCs from three patients with IgM MGUS (ID #11 to #13; table S1) and three with LPL/WM (ID #14 to #16; table S1) to investigate the transcriptional phenotype of clonotypic B cells using an unbiased and holistic approach (Fig. 4A). Predominant BCR gene rearrangements were identified in each case (four were identified in the patient IgM MGUS_2), consistent with clonal B cell expansions under both premalignant and malignant conditions (Fig. 4B). Using gene expression analysis, we classified the clonotypic cells carrying the predominant clonal Ig gene sequence

Table 1. Presence of *MYD88*[L265P] as assessed by WES, ASO-PCR, or dd-PCR in CD34-positive HPCs, B cell precursors, mature B lymphocytes, tumor B cells, and PCs. AFs (per dd-PCR in all cell types and per WES in CD34-positive HPCs, B cell precursors, and mature B lymphocytes) and CCFs (per WES in tumor B cells and PCs) are indicated in parentheses. NT, not tested.

Patient	Method	CD34-positive HPCs	B cell precursors	Mature B lymphocytes	Tumor B cells	PCs
1	WES				(0.56)	(0.39)
	ASO-PCR	positive	positive	positive	positive	positive
	dd-PCR	NT	NT	NT	NT	NT
2	WES			(0.06)	(0.65)	(0.51)
	ASO-PCR	positive	positive	positive	positive	positive
	dd-PCR	NT	NT	NT	NT	NT
3	WES				(0.45)	(0.18)
	ASO-PCR	positive	positive	positive	positive	positive
	dd-PCR	NT	NT	NT	NT	NT
4	WES			NT	(0.55)	(0.04)
	ASO-PCR	positive	positive	NT	positive	positive
	dd-PCR	NT	NT	NT	NT	NT
5	WES			(0.09)	(0.40)	(0.23)
	ASO-PCR	positive	positive	positive	positive	positive
	dd-PCR	NT	NT	NT	NT	NT
6	WES			(0.12)	(0.67)	(0.67)
	ASO-PCR	NT	NT	NT	NT	NT
	dd-PCR			(0.11)	(0.63)	(0.61)
7	WES		(0.05)		(0.49)	(0.44)
	ASO-PCR	NT	NT	NT	NT	NT
	dd-PCR	NT	NT	NT	NT	NT
8	WES			NT	(0.51)	NT
	ASO-PCR	NT	NT	NT	NT	NT
	dd-PCR		(0.16)	NT	(0.46)	NT
9	WES			(0.12)	(0.65)	(0.33)
	ASO-PCR	NT	NT	NT	NT	NT
	dd-PCR		(0.02)	(0.05)	(0.43)	(0.31)
10	WES			NT	(0.57)	(0.40)
	ASO-PCR	NT	NT	NT	NT	NT
	dd-PCR			NT	NT	(0.40)	(0.34)

in each patient into B cell precursors, mature B lymphocytes, and PCs, on the basis of the differential expression of genes such as *CD10* (*MME*), *CD27*, *CD34*, *CD38*, *CD138* (*SDC1*), and *VPREB1*. Clustering analysis of clonotypic cells showed colocalization of B cell precursors and mature B lymphocytes (Fig. 4C and fig. S4). By contrast, the same analysis performed in nonclonotypic cells showed clear segregation of B cell precursors and mature B lymphocytes (Fig. 4D and fig. S5).

Downstream analysis of clonotypic cells showed different distributions across cell maturation stages between premalignant IgM MGUS and LPL/WM (Fig. 4E). In patients with IgM MGUS, most clonotypic cells were confined to the mature B lymphocyte cluster (mean, 96%), whereas the clusters of B cell precursors and PCs had minimal representation (each, mean, 2%). While, in patients with

LPL/WM, most clonotypic cells were also confined to the mature B lymphocyte cluster (mean, 89%), there was a greater fraction of clonotypic cells showing a transcriptional profile overlapping with the B cell precursor cluster (mean, 9%), whereas PCs had a similar, minimal representation (mean, 2%).

Per multidimensional flow cytometry (MFC) immunophenotyping, the percentages of B cell precursors and PCs in patients with IgM MGUS were higher than those above for clonotypic cells with such a gene expression profile (respective means of 27 and 5% per MFC versus 2 and 2% per scRNA/BCR-seq) and nearly identical to the percentages observed with scRNA/BCR-seq considering all clonotypic and nonclonotypic cells (means of 23% B cell precursors and 3% PCs). These results indicate that, in IgM MGUS, most B cell precursors and PCs are polyclonal.
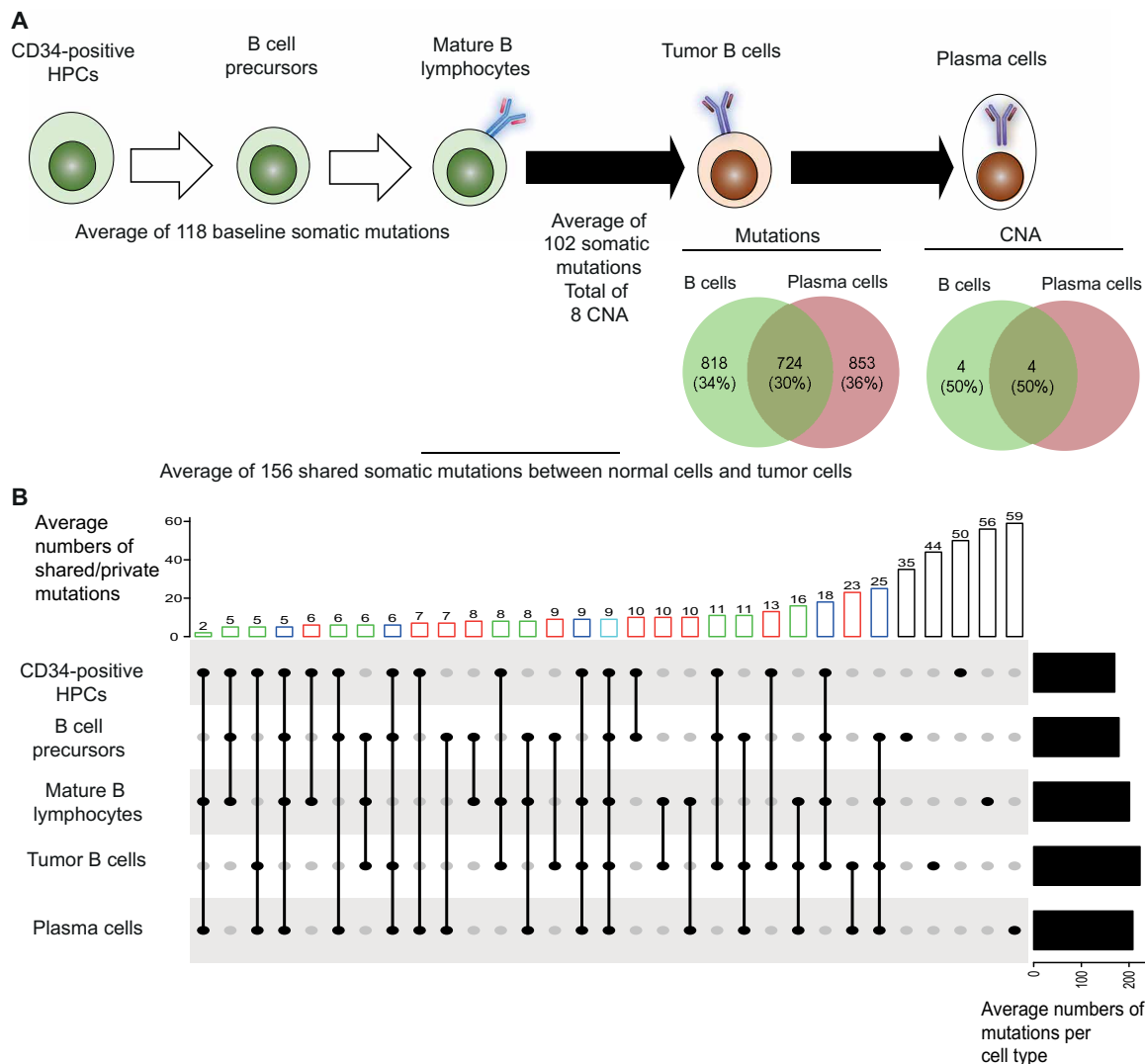
Fig. 3. Genetic evolution during lymphomagenesis: Shared and private somatic mutations in normal cells and tumor cells from patients with LPL/WM ($n = 10$). (**A**) Schematic representation of genetic evolution from CD34-positive HPCs, B cell precursors, and mature B lymphocytes to tumor B cells and PCs. Somatic mutations and CNAs that were private to, or shared between tumor B cells and PCs, are shown in the Venn diagrams. (**B**) UpSet plot summarizing the distribution of somatic mutations present in normal and tumor cells from 10 patients with LPL/WM. Black dots and vertical connecting black lines indicate the sharing of somatic mutations by two or more cell types, represented by the dots. Individual dots represent somatic mutations that are private to the respective cell type. Average numbers of somatic mutations shared by the different combinations of cell types or private to a specific cell type are shown in the top, ordered from lowest to highest number. Bars representing average numbers of somatic mutations shared by two, three, four, or all five cell types are colored red, green, blue, and light blue, respectively. The average numbers of somatic mutations per cell type are indicated on the right side of the plot.

In LPL/WM, high concordance between percentages of cell types per MFC and scRNA/BCR-seq was only observed for PCs (means of 2 and 3%, respectively); accordingly, most PCs were clonal in patients with LPL/WM (Fig. 4E). By contrast, the mean percentage of total B cell precursors per MFC and of clonotypic B cell precursors per scRNA/BCR-seq was 0.4 and 9%, respectively. The mean percentage of total mature B lymphocytes per MFC and of clonotypic mature B lymphocytes per scRNA/BCR-seq was 97.6 and 89%, respectively. Together, these results reveal that, in LPL/WM, a fraction of mature B lymphocytes display an immature gene expression profile. Thus, our findings suggest that progression from IgM MGUS to LPL/WM is associated with the emergence of transcriptionally immature tumor cells. Hence, we observed the significant up-regulation of *CD20* (*MS4A1*) in the gene expression profiles of clonotypic cells in IgM MGUS versus LPL/WM (table S8). We also found deregulation of relevant genes in this disease such as *BCL2*, *CXCR4*, and *HIF1A* (Fig. 4F).

Mutated *MYD88* alone is insufficient to induce lymphoma in mice

If normal progenitor and mature B cells carrying somatic mutations including *MYD88*[L265P] precede the accumulation of additional genetic abnormalities resulting in progression of LPL/WM in humans, then *MYD88*[L265P] induction in mice should, by itself, be insufficient to drive the immediate development of malignancy. To investigate this hypothesis, mice carrying *MYD88*[L252P] (orthologous
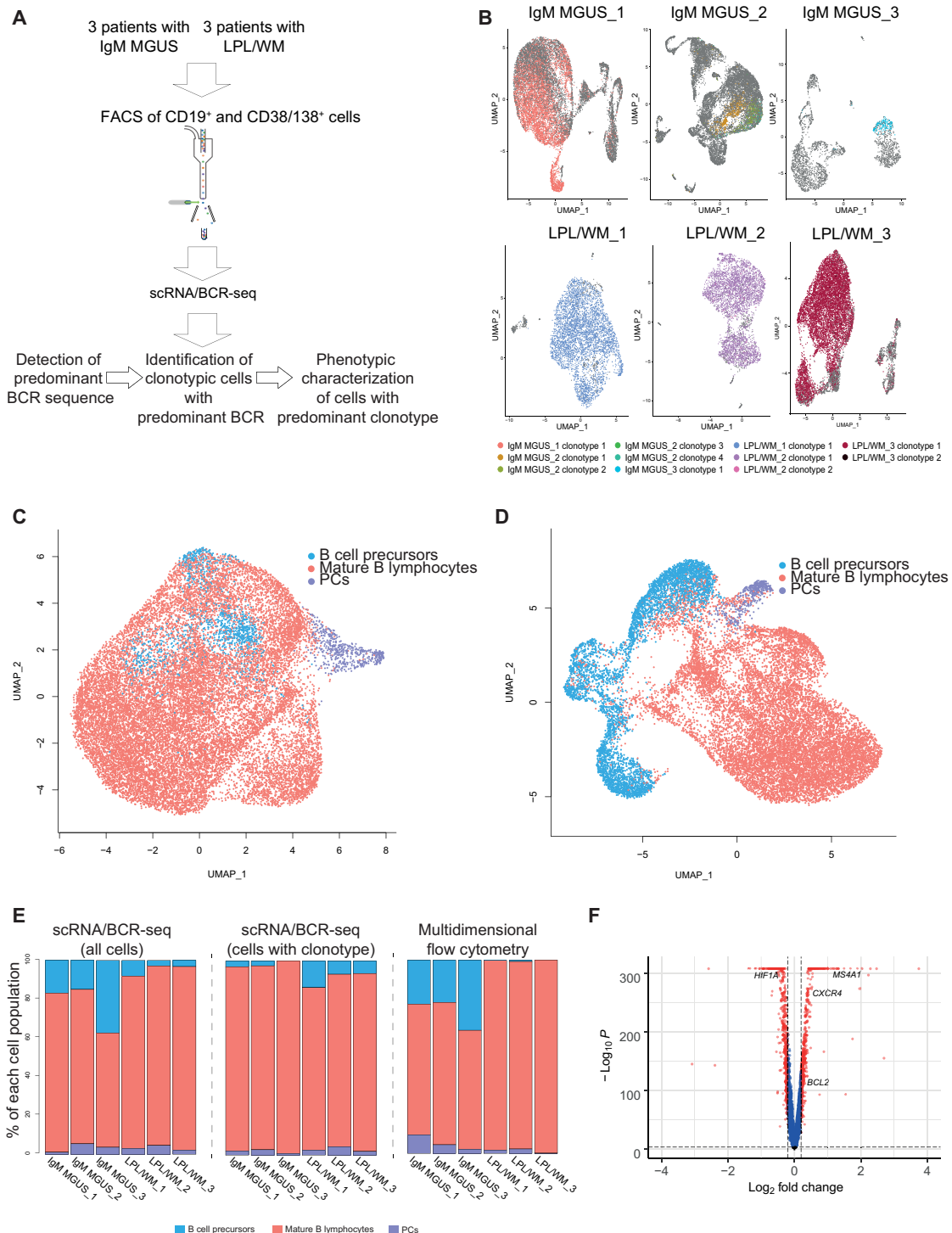
Fig. 4. Intratumor heterogeneity in, and malignant transformation to, LPL/WM. (**A**) Schematic of workflow, including subject disposition, BM cell types isolated by FACS, and methodology used for simultaneous scRNA/BCR-seq. (**B**) Uniform manifold approximation and projection (UMAP) of 42,204 B cells and PCs isolated by FACS from three individuals with IgM MGUS and three patients with LPL/WM. Cells with predominant (clonal) BCR gene rearrangements are represented by specific colors. (**C**) UMAP of cells carrying the clonal Ig gene sequence. B cell precursors, mature B lymphocytes, and PCs are represented by specific colors. (**D**) UMAP of nonclonotypic cells. B cell precursors, mature B lymphocytes, and PCs are represented by specific colors. (**E**) Distribution of cells according to maturation stage (i.e., B cell precursors, mature B lymphocytes, and PCs) based on scRNA/BCR-seq (considering clonotypic plus nonclonotypic cells and only clonotypic cells) and multidimensional flow cytometry (MFC). (**F**) Volcano plot displaying differentially expressed genes found in clonotypic cells from individuals with IgM MGUS and patients with LPL/WM. Each dot corresponds to an individual gene. Differentially expressed genes with a log$_2$ fold change of ≤0.2 and P_{adj} < 0.0005 are colored red. *MS4A1* (*CD20*) is highlighted because of its ascribed role in defining early versus late stages of B cell differentiation. *BCL2*, *CXCR4*, and *HIF1A* are highlighted because of their ascribed role in the pathogenesis of LPL/WM.

to human $MYD88^{L265P}$) were crossed with Sca1-cre, Mb1-cre, and Cγ1-cre mice to selectively activate $MYD88^{L252P}$ in HPCs (M88Ys), B cell precursors (M88Ym), and germinal center (GC) B lymphocytes (M88Yc), respectively (Fig. 5A) (*36*). The Sca1-cre, Mb1-cre, and Cγ1-cre mice carrying the yellow fluorescent protein (YFP) reporter were used as controls (Ys, Ym, and Yc mice, respectively). Because of limited resources, $MYD88^{L252P}$ and control mice were bred independently.

Longitudinal characterization of hematopoietic cell compartments using MFC revealed a moderate expansion of B220$^+$CD138$^+$ plasmablasts and B220$^-$CD138$^+$ PCs in the spleen, as well as B220$^-$CD138$^+$ PCs in the BM in the three models (Fig. 5B). M88Ys, M88Ym, and M88Yc mice had significantly reduced overall survival (OS) versus their respective control mice ($P = 0.0003$, $P = 0.048$, and $P = 0.008$, respectively; Fig. 5C and fig. S6A). There were no significant differences in OS according to sex (fig. S6B). At the time of symptoms or signs of disease, all three models showed hematopoietic cell expansions, which, in M88Ys mice, massively involved the spleen and were of the myelomonocytic lineage (Fig. 5D and fig. S6C). By contrast, M88Ym and M88Yc mice had significantly increased percentages of B220$^+$CD138$^+$ plasmablasts and B220$^-$CD138$^+$ PCs, consistent with the diagnosis of LPL in lymph nodes and salivary glands, although not in the BM (Fig. 5, D to F, and fig. S6D). WES of tumor B cells from M88Ym and M88Yc mice revealed a median of 6.6 CNAs and 97 somatic mutations in addition to $MYD88^{L252P}$. Notably, these somatic mutations were recurrently detected in oncogenes of the BCR/NF-κB signaling cascade (*Card11*, *RelB*, *Nfkbie*, and *Pim1*) and tumor suppressor genes commonly inactivated in lymphoma (*Tp53*, *Pten*, *P16^{INK4a}*, *P15^{INK4b}*, *Gna13*, *Ktm2d*, and *Tnfrsf14*) (table S9). Collectively, these results indicate that genetic alterations in addition to $MYD88^{L252P}$ activation in B cell precursors or mature B lymphocytes are required for the development of LPL in elderly mice.

BCL2 and BCR signaling cooperate with *MYD88* in LPL/WM development in mice

To functionally evaluate which molecular alterations in addition to mutated *MYD88* are required for the development of LPL/WM, which in turn could result in the first experimental model of this disease (*36*, *37*), we crossed the M88Ym model with mice carrying transgenic overexpression in B cells of the antiapoptotic gene *BCL2* (M88B2m), or with EμNKX2.3 (designated BCR) mice that exhibit constitutive BCR signaling (M88BCRm) (Fig. 6A). *BCL2* was selected on the basis of the up-regulation we saw on scRNA/BCR-seq between premalignant IgM MGUS and LPL/WM (Fig. 4F), together with previously published data (*38*, *39*). BCR was selected on the basis of recurrent somatic mutations having been observed in the BCR/NF-κB signaling cascade in M88Ym mice developing LPL and the fact that it is commonly activated in patients with LPL/WM (*27*). *BCL2* and BCR mice were crossed with Mb1-cre mice to respectively generate the B2m and BCRm controls.

M88B2m and M88BCRm mice had significantly inferior OS when compared to M88Ym, B2m, and BCRm mice (median, 11 and 13 months versus 25, 23, and 25 months, respectively; $P < 0.0001$) (Fig. 6B and fig. S7A). No significant differences were found between according to the sex of M88B2m and M88BCRm mice (fig. S7B). In contrast with controls, both M88B2m and M88BCRm mice exhibited nodal and extranodal expansions of B220$^+$CD138$^+$ plasmablasts and B220$^-$CD138$^+$ PCs, similar to those observed in M88Ym mice

(Fig. 6, C to E, and fig. S7, C and D). However, 30% of M88B2m mice that also exhibited BM involvement and LPL development in both M88B2m and M88BCRm mice was associated with increased serum IgM levels (Fig. 6F). Compared to M88Ym and M88Yc mice, tumors from M88B2m and M88BCRm mice had significantly fewer CNAs (median, 1.9 versus 6.6; $P = 0.023$) and somatic mutations (median, 21.5 versus 97; $P = 0.029$), and these did not involve classic oncogenes or tumor suppressors (Fig. 6, G and H, and table S9). Thus, co-occurrence of $MYD88^{L252P}$ and *BCL2* overexpression or constitutive BCR signaling accelerated the development of LPL, which consequently accumulated fewer (nonspecific) genetic alterations. *BCL2* overexpression as a secondary event reflected some key features of human LPL/WM such as BM involvement and IgM secretion (*29*).

Monitoring treatment efficacy based on the presence of $MYD88^{L265P}$

Detection of $MYD88^{L265P}$ by dd-PCR has been suggested as a highly sensitive method for monitoring treatment efficacy in LPL/WM (*34*). However, we observed a subclonal presence of $MYD88^{L265P}$ in sporadic cases (e.g., patient #4; table S4) and wild-type *MYD88* in some tumor cells carrying other genetic lesions (Fig. 7A), which could produce false-negative results. Moreover, the unexpected finding of $MYD88^{L265P}$ in normal precursor and mature B lymphocytes of patients with LPL/WM could produce false-positive results. Thus, we hypothesized that these results have possible clinical sequelae by limiting the utility of $MYD88^{L265P}$ for monitoring treatment efficacy.

To investigate this, we analyzed the prognostic significance of treatment response according to $MYD88^{L265P}$ status by ASO-PCR in whole BM aspirates from 46 patients with LPL/WM (table S10). There were no significant differences in time to progression (TTP) between patients who were ASO-PCR–negative ($n = 20$, 43.5%) versus ASO-PCR–positive ($n = 26$, 56.5%) for $MYD88^{L265P}$ (median of 27 months versus 33 months, respectively; $P = 0.787$) (Fig. 7B). We also analyzed, in the same cohort, the prognostic significance of treatment response per MFC, which monitors phenotypically aberrant and light chain–restricted clonal B cells. Patients with ≤0.1% clonal B cells ($n = 14$, 30.4%) had median TTP not reached, whereas cases with ≥0.1% clonal B cells ($n = 32$, 69.6%) showed a median TTP of 33 months ($P = 0.192$) (Fig. 7C). There was 73.9% concordance between methods, with 11 (23.9%) patients negative and 23 (50%) patients positive by both techniques. Three (6.5%) patients were ASO-PCR–positive/MFC-negative and nine (19.6%) were ASO-PCR–negative/MFC-positive (Fig. 7D). Together, these results suggest limited concordance between the presence of tumor B cells and $MYD88^{L265P}$ status in whole BM aspirates and the limited prognostic value of this genetic marker for measuring treatment efficacy.

DISCUSSION

The genomes of thousands of tumors have been elucidated (*40*, *41*), but information about somatic genetic alterations in normal cells remains limited, and it is only recently that data have shown that normal cell counterparts of various solid tumors accumulate several mutation years before disease onset (*2–5*). Evidence showing that normal B lymphocytes carry genomic alterations outside the Ig loci is even more limited, and the role of these mutations in lymphomagenesis is virtually unknown (*18–20*). To our knowledge, the work
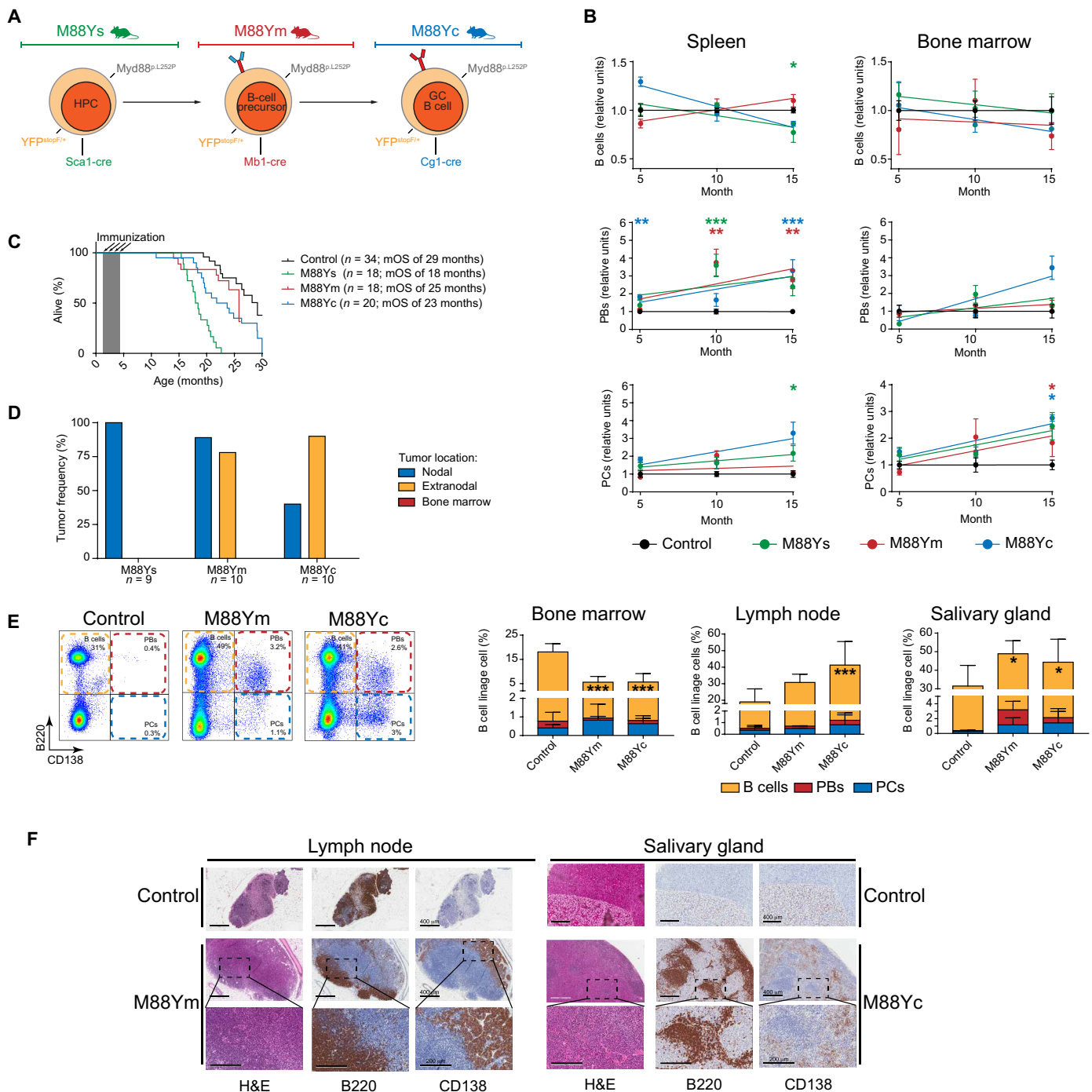
Fig. 5. Mutated *MYD88* alone is insufficient to induce lymphoma in mice. (**A**) Schematic representation of the transgenic mouse models used in these experiments. (**B**) Relative numbers (versus controls) of B cells, plasmablasts (PBs), and PCs in the spleen and BM of mice euthanized at 5, 10, and 15 months of age (*n* = 6 mice per cohort); *P < 0.05, **P < 0.01, and ***P < 0.001. (**C**) Kaplan-Meier distributions of overall survival (OS) for the three transgenic mouse models and control mice, plus median OS (mOS) for each. (**D**) Frequencies of tumor locations in the three transgenic mouse models. (**E**) Flow cytometry analyses showing the percentages of B cells, plasmablasts, and PCs in the BM, lymph nodes, and salivary glands of control mice and the M88Ym and M88Yc mouse models (*n* = 6 mice per cohort); *P < 0.05 and ***P < 0.001. Data were obtained from M88Ym and M88Yc mice euthanized upon symptoms or signs of disease (between 18 and 24 months) and were compared with age-matched Ym and Yc mouse controls. (**F**) Representative histopathologic staining with hematoxylin and eosin (H&E) and B220 and CD138 mAbs in lymph nodes from M88Ym mice and in salivary glands from M88Yc mice.
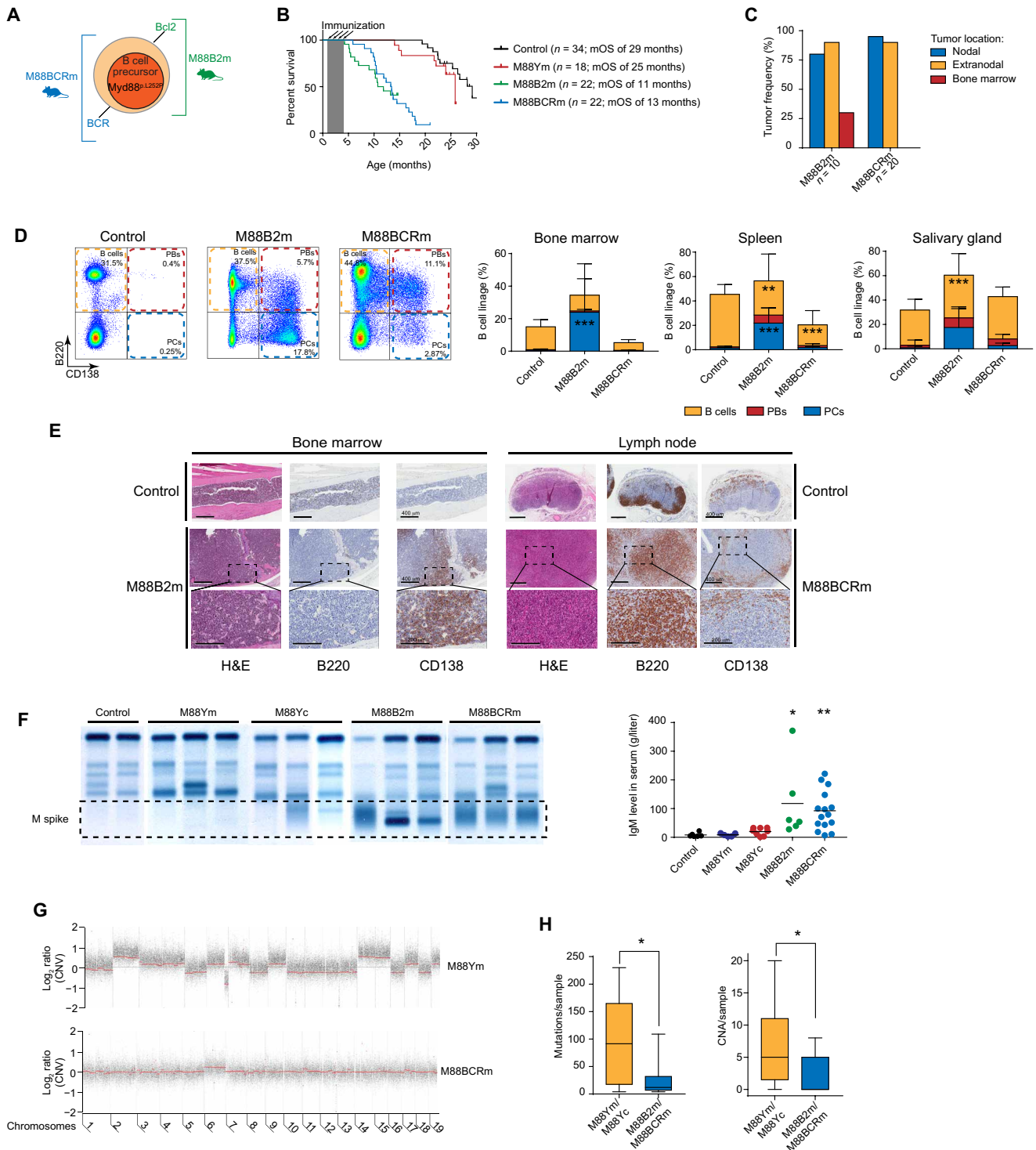
Fig. 6. *BCL2* and BCR signaling cooperate with *MYD88* in LPL/WM development in mice. (**A**) Schematic representation of M88B2m and M88BCRm transgenic mice. (**B**) Kaplan-Meier distributions of OS for M88B2m, M88BCRm, M88Ym, and control mice, plus median OS for each. (**C**) Frequencies of tumor locations in M88B2m and M88BCRm transgenic mice. (**D**) Flow cytometry analyses showing the percentages of B cells, plasmablasts, and PCs in the BM, lymph nodes, and salivary glands of M88B2m and M88BCRm mice versus control mice (n = 6 mice per cohort); **P < 0.01 and ***P < 0.001. (**E**) Representative histopathologic staining with hematoxylin and eosin and B220 and CD138 mAbs in the BM of M88B2m mice and in lymph nodes of M88BCRm mice. (**F**) Serum electrophoresis and IgM levels by enzyme-linked immunosorbent assay in M88B2m and M88BCRm mice compared to M88Ym, M88Yc, and control mice; *P < 0.05 and **P < 0.01. (**G** and **H**) Median number of CNAs (G) and somatic mutations (H) per tumor in mice with single *MYD88* mutation (M88Ym and M88Yc) versus those with *MYD88* mutation and secondary genetic alterations (M88B2m and M88BCRm); *P < 0.05.
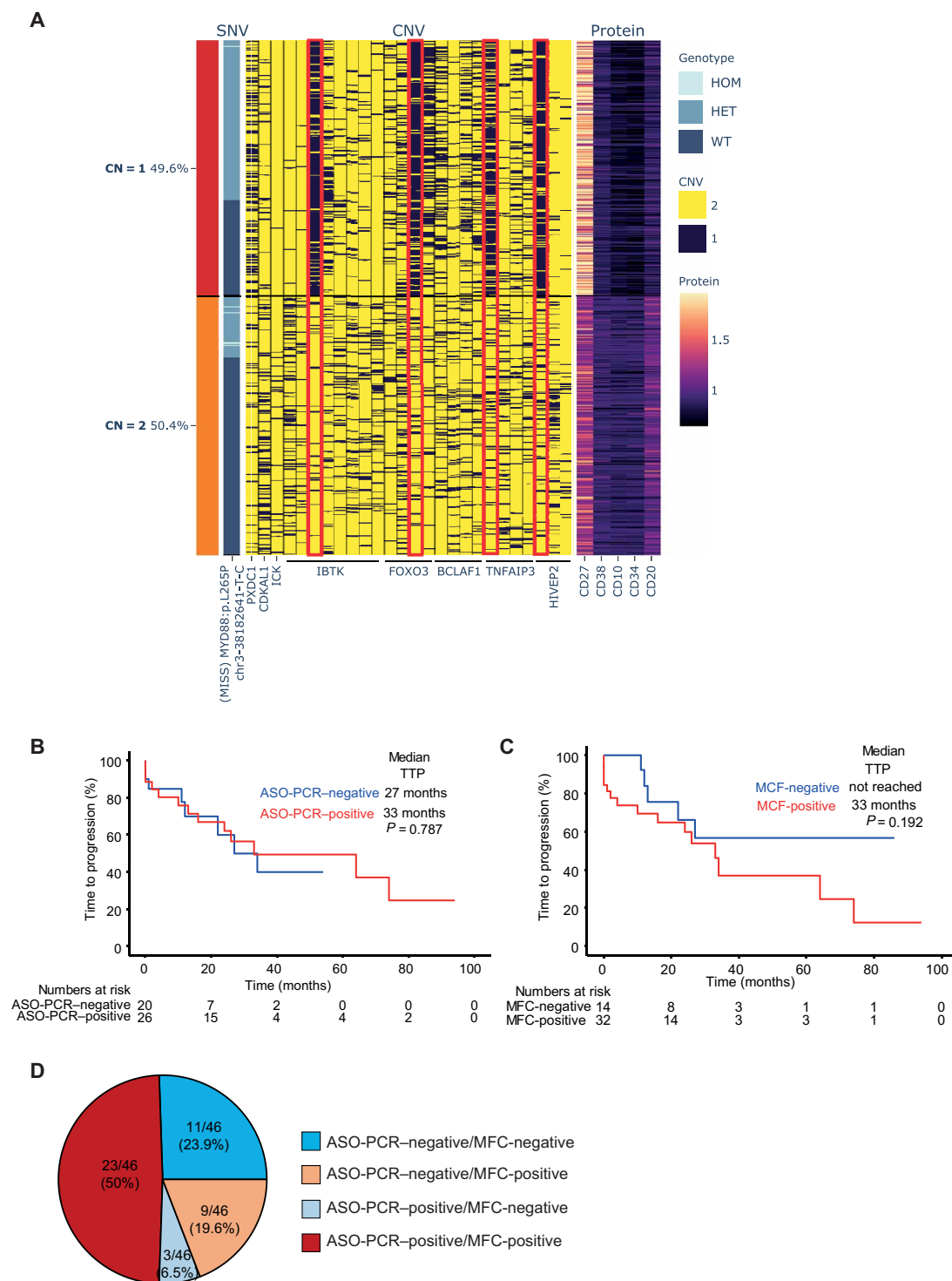
Fig. 7. Monitoring treatment efficacy based on the presence of *MYD88*^{L265P}. (**A**) Mature B lymphocytes ($n = 2497$) from one patient with LPL/WM, showing wild-type *MYD88* and CNAs in selected regulatory regions of 6q, per scDNA-seq. (**B** and **C**) Kaplan-Meier distributions of time to progression (TTP) from time of response assessment, according to presence versus absence on ASO-PCR of *MYD88*^{L265P} in whole BM samples after treatment (B) and presence versus absence of ≥0.1% phenotypically aberrant B cells on MFC (C). (**D**) Number and proportion of patients with LPL/WM ($N = 46$) who were positive or negative for *MYD88*^{L265P} on ASO-PCR and did or did not have ≥0.1% phenotypically aberrant B cells on MFC.

reported herein is the first time that somatic mutation landscapes in BM CD34-positive HPCs, B cell precursors, and mature B lymphocytes from elderly individuals and patients with LPL/WM have been characterized. On the basis of our comprehensive set of experiments, evaluating human cells and mouse models and using multiple analytical techniques, we have demonstrated that a mutation in a gene relevant to B cell function, such as *MYD88*, represents a preneoplastic event that requires additional genetic alterations to drive lymphomagenesis. Consequently, we conclude that $MYD88^{L265P}$ alone does not conduce to overt malignant transformation.

The presence of somatic mutations in mature B lymphocytes has been primarily attributed to the DNA mutator activation-induced cytidine deaminase during GC reactions. However, we found that most somatic mutations are detected outside the Ig loci and that a fraction of these originate in immature B cell precursors and even CD34-positive HPCs. Conversely, we found that most somatic mutations detected in progenitor cells were undetectable in mature B lymphocytes, suggesting negative selection of these clones during B cell lymphopoiesis. Our data from normal cell types from elderly individuals and patients with LPL/WM therefore support the idea that most spontaneous somatic mutations are harmless, unless they hit genes such as *MYD88*.

The pathogenesis of LPL/WM is characterized by recurrent somatic mutations in *MYD88* and *CXCR4*, together with deletions in chromosome 6q that affect regulatory genes (*27*, *42*). However, it remains unclear which of these genetic alterations appear before the development of overt disease or how they evolve. Our study establishes a preneoplastic landscape of mutations, including $MYD88^{L265P}$, in the B lineage of patients with LPL/WM. These findings are not contradictory with the role of this hotspot mutation in lymphomagenesis or the importance of $MYD88^{L265P}$ activity in tumor cells (*43*, *44*). However, our results suggest that the contribution of $MYD88^{L265P}$ to tumor initiation is limited in the absence of additional genetic alterations. Accordingly, progression to LPL/WM from clonal lymphopoiesis was systematically preceded by the acquisition of new genetic abnormalities.

Our study was not powered to determine which specific mutations, allele burdens, or patterns of coexisting genetic alterations trigger the progression to LPL/WM. Nevertheless, our data provide further support for mutations in *CXCR4* or in pan-cancer genes (e.g., *TP53* and *DICER1*), together with CNAs, particularly del(6q), being required for the expansion of clonal cells with the LPL/WM phenotype (*29*, *45–48*). Furthermore, it could be hypothesized that, if these cooperating events hit an IgM-positive B lymphocyte that has been recently activated in a GC and that shows a high expression of the α chain receptor of interleukin-2 (i.e., CD25) (*33*), these mutations would specifically result in progression to LPL/WM, rather than another lymphoma that may present with $MYD88^{L265P}$ (*28*).

Although a number of myeloid disorders are known to arise at the HPC level, most hematologic malignancies have been linked to later stages of differentiation (*49*). Mature B cell disorders are the most common types of blood cancer and are classified according to their presumed cell of origin in the continuum of B cell development (*49*). That notwithstanding, HPCs from patients with CLL have been shown to have a cell-intrinsic propensity to generate clonal CLL-like B cells (*21*), which could help explain the presence of shared somatic mutations in tumor cells and CD34-positive HPCs from patients with CLL (*23*, *24*). Similarly, $BRAF^{V600E}$ mutations in hairy cell leukemia (HCL) were derived from an HPC origin

(*22*), strengthening the notion that even driver mutations may occur in CD34-positive HPCs before malignant transformation in some B cell disorders. In our study, we showed that $MYD88^{L265P}$ at the HPC level was infrequent and that it was highly unlikely that these act as cancer stem cells (CSCs) because of the extremely low probability of these cells giving rise repeatedly to tumor cells carrying the same stepwise-acquired genetic abnormalities. In addition, we showed that LPL/WM clones comprise multiple subsets, including cells with transcriptional profiles similar to those of B cell precursors. Thus, our study sheds new light on the question of whether CSCs are derived from true stem cells or mature cells that have undergone a dedifferentiation process (*50*, *51*), and we propose a model in which predisposition due to clonal lymphopoiesis coexists with the intratumor heterogeneity of immature and mature clusters.

Previously, it has been reported (*36*) that a knock-in mouse model carrying endogenous mouse $MYD88^{L252P}$ developed DLBCL infrequently, and with long latency, but not a B cell disorder with the morphologic features of LPL/WM. More recently, transgenic mice expressing the human $MYD88^{L265P}$ gene in GC and post-GC B cells have been generated (*37*); the authors concluded that $MYD88^{L265P}$ alone was insufficient to drive malignant transformation but that it did promote a nonclonal, low-grade B cell expansion with some clinicopathologic features resembling LPL/WM (*37*). As with mouse models with endogenous $MYD88^{L252P}$, $MYD88^{L265P}$ transgenic mice occasionally developed DLBCL harboring secondary mutations and expressing BCL6 (*37*). We expanded on these previous results by inducing $MYD88^{L252P}$ in mouse HPCs, B cell precursors, and GC B lymphocytes to simulate its presence in immature and mature cells of the B lineage found in patients with LPL/WM. Our results showed that mutated *MYD88* induced an expansion of lymphoplasmacytic cells and revealed that accumulation of plasmablasts and PCs was more evident in mice with activation of mutated *MYD88* in B cell precursors versus GC B lymphocytes. However, these findings do not indicate that $MYD88^{L252P}$ must occur before GC to drive disease development, and recent data by Schmidt *et al.* (*52*) support the notion that an expansion of IgM expressing PCs can be observed if the mutation is introduced early or at late stages during B cell development. Furthermore, in our models, as well as in that of Ouk *et al.* (*53*), full-blown LPL was seen only with long latency and only at nodal or extranodal sites, without the BM infiltration seen in patients with LPL/WM. Similar findings have been reported in HCL: After detection of $BRAF^{V600E}$ in HPCs from patients with HCL, it was shown that expression of $BRAF^{V600E}$ in murine HPCs resulted in increased clonogenic capacity of early B cell populations, but not in the expansion of cells with the HCL phenotype (*22*).

These studies all support the principle that additional co-occurring genetic alterations during the course of hematopoiesis (e.g., $CXCR4^{WHIM}$) are necessary to produce malignant lymphoplasmacytic cells that infiltrate the BM (*27*). Accordingly, we showed that mutations in genes that co-occur with $MYD88^{L265P}$ in patients with LPL/WM, such as *CXCR4*, *ARID1A*, and *CD79b*, were not among the numerous somatic mutations found in mice developing nodal or extranodal LPL. Notably, these mutations may have been acquired following (and hence not required for) disease onset. However, we demonstrated that *MYD88* mutation and two secondary events (i.e., *BCL2* overexpression and constitutive BCR signaling) cooperated to accelerate the clonal expansion of lymphoplasmacytic cells that required the accumulation of fewer genetic abnormalities, secreted IgM paraprotein, and infiltrated the BM in mice with *BCL2*

overexpression. These findings resemble some of the key biologic, genetic, and clinical features of LPL/WM in patients and are consistent with the importance of del(6q) together with $MYD88^{L252P}$ in LPL/WM pathogenesis, as the loss of genes that repress BCL2 activity (e.g., *BCLAF1*) is a consequence of del(6q) (*54, 55*). Conversely, other cooperating events, such as augmented HOIP (oxidized IRP2 ubiquitin ligase-1-interacting protein) expression, may facilitate DLBCL-like B cell lymphomagenesis driven by *MYD88*-activating mutation(*56*). Thus, our study builds upon previous *MYD88* mutant mouse models, in such a way that the results of bulk and single-cell sequencing studies in elderly individuals and patients allowed us to identify the genetic events necessary for the development of tumors resembling LPL/WM in mice. These can be valuable models to test the efficacy of newer combinations including drugs such as ibrutinib and venetoclax.

It is important to translate knowledge obtained from genomic research into clinical practice. The high frequency of $MYD88^{L265P}$ in LPL/WM, together with the ability to monitor this mutation using high-sensitivity methods such as dd-PCR (*34*), suggests a role for $MYD88^{L265P}$ as a biomarker for evaluating treatment efficacy (*28*). However, the presence of $MYD88^{L265P}$ in phenotypically normal cells that do not drive progression to LPL/WM could confound interpretation of therapeutic response based on the presence of $MYD88^{L265P}$. Our TTP data showed that patient stratification based on detection of mutated *MYD88* using ASO-PCR in whole BM samples was not predictive of disease-free survival (*57, 58*). This could be related to false positives on ASO-PCR due to $MYD88^{L265P}$ clonal lymphopoiesis in a subset of patients. Our results could also shed light on some unexpected findings in treated LPL/WM (*59, 60*), which showed that some patients had $MYD88^{L265P}$ in unselected BM samples but not in CD19-positive sorted cells. Similar observations have been reported in cases with chronic myeloid leukemia; the presence of *BCR-ABL1* mRNA in peripheral blood from patients in treatment-free remission was seen predominantly in the B cell compartment and thus did not imply the persistence of multipotent leukemic cells (*61*). Accordingly, it could be hypothesized that, similar to what is seen in acute myeloid leukemia, which is also preceded by clonal hematopoiesis (*62*), optimal monitoring of treatment efficacy in LPL/WM may require the use of both molecular and immunophenotypic methods (*46*). Because our small series was underpowered to provide conclusive evidence, further studies are warranted to confirm this hypothesis and to increase the sensitivity of MFC to levels achieved in other hematological malignancies (*63, 64*).

LPL/WM represents a pivotal example of a blood cancer in which improved understanding of the underlying genetic abnormalities has had a profound effect on differential diagnosis, responsiveness to treatment, and outcome (*27*). Through the studies reported here, we have built upon these seminal observations. We have shown that $MYD88^{L265P}$ arising during hematopoietic development could represent a unifying event in progression to LPL/WM, albeit one that does not always occur at the same cellular stage. We have also shown that stepwise acquisition of secondary events additional to $MYD88^{L265P}$ occurs during progression to LPL/WM and that this varies considerably across patients. Because additional genetic hits may affect all or only a fraction of tumor cells, this stepwise acquisition would explain the intraclonal heterogeneity seen in full-blown LPL/WM, including transcriptionally immature clusters. Furthermore, our results could support a role for high-sensitivity monitoring of $MYD88^{L265P}$ in the B cell lineage of healthy elderly individuals to enable early identification of those at risk of developing LPL/WM and potentially other *MYD88*-mutated lymphoma.

MATERIALS AND METHODS
Subjects, patients, and samples collected
In this study, we analyzed 117 cell samples/cell types isolated from 54 BM aspirates obtained from 3 individuals with IgM MGUS, 46 patients with LPL/WM (diagnosed according to World Health Organization criteria), and 5 elderly individuals undergoing orthopedic surgery. The latter had no medical history of cancer. All subjects provided written informed consent before BM aspirate sample collection and analysis; study procedures followed the recommendations and guidelines of the local ethics committee and the Declaration of Helsinki. Patients were enrolled in five institutions (Clinica Universidad de Navarra, Hospital Universitario de Salamanca, Centro Hospitalar e Universitario de Coimbra, Hospital de S. Teotónio, and ASST Spedali Civili di Brescia). Samples (i.e., diagnostic left-overs) were selected after diagnostic flow cytometry immunophenotyping was performed in BM aspirates, which were collected after clinical suspicion of an IgM MGUS and/or LPL/WM. The identification of tumor cells by flow cytometry triggered cell sorting according to the project workflow, and a subsequent confirmation of $MYD88^{L265P}$ by diagnostic molecular testing was a prerequisite for the final selection of patients into the study. A complete list of all cell types isolated from each subject and methodologies used in each case is available in table S1; patient' characteristics are described in table S11. The study was evaluated by the Universidad de Navarra ethics committee [E34-20(076c-17E1)].

Generation of MYD88$^{p.L252P}$ transgenic mice
$MYD88^{p.L252P}$ transgenic mice (hereafter abbreviated as M88) and Sca1^{-Cre} mice (designated as s) have been previously reported (*36, 65*). Mb1^{-Cre} mice (designated as m) were obtained from Reth and co-workers (*66*). Cγ1^{-Cre} mice (stock #010611) (designated as c) and *R26-stop-EYFP* mice (stock #006148) (designated as Y, which facilitated monitoring and isolation of transgenic B cells) were obtained from the Jackson Laboratory (*67, 68*). Compound mice were generated by crossing M88 mice with Y mice to create the M88Y line, which was then crossed with each of the s, m, and c mice to induce specific transgenic activation in HPCs (M88Ys mice), pre–B cell precursors (M88Ym mice), and mature GC B cells (M88Yc mice). As controls, Y mice were crossed with the corresponding cre-recombinase mice to generate Ys, Ym, and Yc mice. To generate transgenic lines with two specific genetic changes, M88Ym mice were crossed with EµBCL2 mice (bcl-2-22 strain; 002319 from the Jackson Laboratory) and with EµNKX2.3 mice (*69*) to generate M88B2m and M88BCRm mice, respectively. In the NKX2.3 model, the overexpression of this homebox gene in B cells induces a constitutive phosphorylation of the Syk/Lyn kinases and the subsequent activation of the BCR pathway, which is followed by the activation of chemokines, adhesion molecules, and integrins that promotes B cell migration to splenic and other extranodal tissues, eventually leading to a malignant transformation that recapitulates features of human marginal zone B cell lymphomas (*69*). All transgenic alleles were maintained in heterozygosity.

To ensure transgenic activation in mature B lymphocytes, 8- to 10-week-old mice were immunized with sheep red blood cells administered intraperitoneally every 3 weeks for four doses. Then,

mice from each cohort (n = 5) were euthanized and necropsied at 5, 10, and 15 months of age and characterized (see below). At least 20 mice from each cohort generated through multiple desynchronized parallel breeding pairs were monitored beyond the age of 15 months and euthanized when signs of disease became present. Mice were housed in specific pathogen–free animal facilities of the Center for Applied Medical Research. All procedures were approved by the local ethical committee of animal experimentation and the Navarra health department [E34-20(076c-17E1)].

MFC immunophenotyping and FACS
EDTA-anticoagulated BM aspirates were stained with the following combination of mAbs before FACS: CD20-PacB, CD27-OC515, surface IgM (suIgM)–fluorescein isothiocyanate (FITC), CD305-PE, CD34-PerCPCy5.5, CD19-PECy7, CD25-APC, and CD38-APCH7. This combination of mAbs enabled the identification and simultaneous isolation of CD34-positive HPCs (CD19-negative, CD20-negative, CD34^{hi}), B cell precursors (CD19-positive, CD20-heterogeneous, CD34-heterogeneous, CD38^{hi}), normal mature B lymphocytes (CD19-positive, CD20^{hi}, CD305-positive, CD27-heterogeneous, CD25-negative, suIgM-negative], tumor cells (CD19-positive, CD20^{hi}, CD25-positive, CD27-positive, CD305-negative, suIgM-positive), PCs (CD38^{hi}, intermediate scatter), and T/NK cells (CD19-negative, CD20-negative, low scatter) (fig. S1). Cells were isolated in a FACSAria IIb flow cytometer [BD Biosciences (BDB), San Jose, CA] and sorted into 100 µl of Lysis/Binding Buffer (Thermo Fisher Scientific, Waltham, MA) for subsequent bulk sequencing or into phosphate-buffered saline (PBS)/bovine serum albumin for single-cell studies.

In the cohort of 46 patients with LPL/WM in whom TTP was evaluated according to presence of $MYD88^{L265P}$, response to induction therapy was assessed by MFC using the following combination of mAbs: CD138-BV421, CD27-BV510, suIgM-FITC, CD25-PE, CD22-PerCPCy5.5, CD19-PECY7, cyκ-APC, and cyλ-APCH7. BM samples were collected in EDTA-containing tubes and processed within 24 hours following the EuroFlow lyse-wash-stain protocol (45). Data acquisition was performed in a FACSCanto II flow cytometer (BDB) using FACSDiva 8.0.1 software (BDB). Data analysis was performed using Infinicyt software (Cytognos SL, Salamanca, Spain). The limit of detection of tumor cells is 0.1%, and, therefore, this was the cutoff used to define patients with negative (<0.1%) or positive (≥0.1%) MFC after treatment.

For analysis of BM and tumor tissue samples obtained from mice, the following marker combinations were used to define B lymphocytes (B220$^+$CD138$^-$), plasmablasts (B220$^+$CD138$^+$), PCs (B220$^-$CD138$^+$), T cells (CD3$^+$CD4$^+$ and CD3$^+$CD8$^+$), myeloid cells (CD11b$^+$Ly6G/Ly6C$^+$, CD11b$^+$Ly6G/Ly6C$^-$, and CD11b$^-$Ly6G/Ly6C$^+$), and nonmyeloid cells (CD11b$^-$Ly6G/Ly6C$^-$). Fc block was used to prevent nonspecific binding of Fc receptor. PBS was added to each sample, and samples were centrifuged for 5 min at 1500 rpm. Supernatant was decanted, and cells were stained with 7-AAD (7-aminoactinomicina D) to assess cell viability (1:100 dilution in PBS) for 5 min at room temperature. Samples were measured in a FACSCantoII flow cytometer (BDB), and data were analyzed using FlowJo software (BDB). B cells were sorted on a FACSAriaII flow cytometer (BDB) and collected for WES.

WES and data analysis
WES was performed on a total of 78 cell samples per cell types, including tumor and normal cells from 10 patients with LPL/WM,

normal cell subsets from five elderly individuals, and T/NK cells (used as germline controls) from all subjects. DNA was purified using AMPure XP magnetic beads (Beckman Coulter Life Sciences, Indianapolis, IN), and its quality was evaluated in an Agilent 4200 TapeStation using the Genomic DNA ScreenTape system (Agilent, Santa Clara, CA). DNA concentration was quantified using the Qubit System (Invitrogen, Carlsbad, CA). WES was performed with molecular barcoding because of the relatively low numbers of normal cells isolated; median numbers of cells sorted per subject were 20,005 CD34-positive HPCs, 15,420 B cell precursors, 31,837 normal mature B lymphocytes, 92,700 tumor cells, 10,099 PCs, and 100,000 T/NK cells. Genomic DNA (approximately 1.0 to 1.75 ng) was captured for each sample in a 10X Chromium instrument using the Chromium Genome Reagent Kit V2 for Exome Assays (10X Genomics, Pleasanton, CA). DNA was then fragmented to an average size of 225 base pairs using a Covaris S220 ultrasonicator (Covaris, Woburn, MA) and subjected to DNA library construction using the Chromium Genome Reagent Kit V2 for Exome Assays (10X Genomics). Target enrichment was performed with the SureSelectXT Human All Exon V6 Capture Library (Agilent), and sequence targets were captured and amplified in accordance with the manufacturer's recommendations. Enriched libraries were used for 150 base sequencing in NovaSeq 6000 (Illumina, San Diego, CA) in accordance with the manufacturer's instructions. Sequencing resulted in a mean read depth of 112× (range, 33 to 216×).

Raw FASTQ files were processed using LongRanger (v2.2.2, 10X Genomics) (70) with default parameters. Variants were annotated using the bioinformatics software HD Genome One (DREAMgenics, Oviedo, Spain), as well as using several databases containing functional (Ensembl, CCDS, RefSeq, and Pfam), populational (dbSNP, 1000 Genomes, ESP6500, and ExAC), and cancer-related (COSMIC release 87 and ICGC release 27) information. In addition, nine scores from algorithms for the prediction of the impact caused by nonsynonymous variants on the structure and function of the protein were used (SIFT, PROVEAN, MutationAssessor, MutationTaster, LRT, MetaLR, MetaSVM, FATHMM, and FATHMM-MKL) (71–77), and one score (GERP++) for evolutionary conservation of the affected nucleotide was used (78). Indel realignment was performed to correct underestimated AFs. Variants with a population AF of >0.01 were excluded. Variants detected in all cell types, including T/NK cells, as well as variants with an AF of >0.25 in T/NK cells, were excluded. Only mutations with a coverage of >10 in all samples from an individual subject were selected. Only variants detected in a sample with a mutated allele count of ≥3 and a droplet count of ≥3 were selected. The detection of CNAs was performed using a modified version of the exome2cnv algorithm (79), incorporating a combination of read depth and allelic imbalance computations for CNA assessment. For each patient, the algorithm uses its control sample as background for computing CNA (79). Distribution of mutations across the genome was represented with rainfall plots using karyoploteR R package (80). An UpSet plot was developed to visualize the distribution of somatic mutations present in multiple cell types using the ComplexHeatmap R package (81). CCFs were calculated with the cDriver R package (82).

WES was performed on tumor samples obtained from 8 M88Ym/M88Yc mice and 15 M88B2m/M88BCRm mice and on 10 samples of normal cells from control mice. Genomic DNA was purified using the NucleoSpin Tissue Kit (Macherey-Nagel), according to the manufacturer's instructions. DNA concentration and integrity were

evaluated as described above. Exome capture libraries were prepared per the instructions of the SureSelectXT mouse all exon target enrichment system (Agilent Technologies). Exome libraries were sequenced using a 151–base pair paired-end read protocol on an Illumina NovaSeq 6000.

ASO-PCR and dd-PCR

The presence of $MYD88^{L265P}$ was assessed using ASO-PCR ($N = 5$) or dd-PCR ($N = 4$) according to whether a higher or lower amount of DNA, respectively, was left over after WES. In 1 of the 10 patients with LPL/WM in whom WES was performed, there was no DNA available for the confirmatory analysis by PCR. ASO-PCR and dd-PCR were performed using the methodology validated elsewhere (*34, 83*). In the cohort of 46 patients with LPL/WM in whom TTP was evaluated according to presence of $MYD88^{L265P}$, the limit of detection of ASO-PCR was 0.1%.

scRNA/BCR-seq and analysis

All B cells and PCs isolated by FACS on the basis of high expression levels of CD19 and of CD38 plus CD138 (median of 4132 cells per patient), respectively, were simultaneously isolated into a single aliquot. scRNA/BCR-seq was performed using 10X Genomics Single Cell 5′ Solution, version 2, according to the manufacturer's instructions (10X Genomics). Libraries were sequenced on NextSeq 550 (Illumina) and analyzed using the Cell Ranger version 3.0.0 software (10X Genomics). Quality control metrics were used to select cells with mitochondrial genes representing <10% of total genes and with at least 2500 genes. Samples were analyzed using Seurat (https://satijalab.org/seurat/). Clonotypic BCR Ig gene rearrangements were defined on the basis of their presence in 10 or more cells. To integrate different scRNA/BCR-seq samples, we used a normalization and variance stabilization of molecular count data based on regularized negative binomial regression with a sctransform function (*84*). Differentially expressed genes between clonotypic cells from patients with IgM MGUS and LPL/WM were identified using Wilcoxon rank sum test.

scDNA-seq and analysis

CD34-positive HPCs, B cells, and PCs from BM samples obtained from four patients with LPL/WM were simultaneously isolated by FACS into a single aliquot. A pool of six oligo-conjugated antibodies from Mission Bio Inc. (CD10, CD20, CD27, CD34, and CD38) was then added, followed by incubation for 30 min at room temperature. Cells were washed with Dulbecco's PBS supplemented with 5% fetal bovine serum (Gibco), which was followed by resuspension in Tapestri cell buffer, quantification, and loading of the cells into a Tapestri microfluidics cartridge (Mission Bio, San Francisco, CA) for subsequent encapsulation, lysis, and barcoding. Barcoded samples were then subjected to targeted PCR amplification of a custom set of 29 amplicons covering *CD79b*, *CXCR4*, *MYD88*, and genes with regulatory functions in chromosome 6q (table S12). DNA PCR products were then isolated from individual droplets, purified with AMPure XP beads, used as a PCR template for library generation, and purified using AMPure XP beads. Protein PCR products were incubated with Tapestri pullout oligo (5 μM) at 96°C for 5 min, followed by incubation on ice for 5 min. Protein PCR products were then purified using streptavidin C1 beads (Invitrogen), and beads were used as a PCR template for the incorporation of i5/i7 Illumina indices, followed by purification using AMPure XP beads. All libraries, both DNA and protein, were quantified using an Agilent Bioanalyzer and pooled for sequencing on a HiSeq X (Illumina) with 150–base pair ending multiplexed runs.

FASTQ files generated by the sequencer were processed using the Tapestri Pipeline V2 and included adapter trimming, sequence alignment (Burrows-Wheeler Aligner) to human genome (GRCh37/hg19), barcode correction, cell finding, and variant calling (Genome Analysis Toolkit v4/HaplotypeCaller). Loom and h5 files were then processed with Tapestri Insights v2.2 (variant selection) and the Python-based Mosaic package (multiomics analysis and data visualization).

Tapestri Insights analysis used default filter criteria (e.g., genotype quality ≥ 30, reads/cell/target ≥ 10, and mutant VAF $\geq 20\%$) and annotation-based information [e.g., ClinVar and DANN(deleterious annotation of genetic variants using neural networks)]. Only cells with complete genotype information for all variants that were used for downstream analysis were included. Cells that did not satisfy these criteria were considered to have missing genotypes.

Characterization of MYD88^{P.L252P} transgenic mice

Blood samples were extracted from mice at the time of euthanasia, collected in Microvette 55 Z-Gel tubes (Sarstedt, reference 20.1344), and centrifuged at 10,000*g* for 5 min at room temperature. After centrifugation, serum was recovered, and electrophoresis was performed in Hydragel Protein(E) agarose gel (Selbia). BM and spleen tissue samples were disaggregated mechanically and filtered in 70-μm cell strainers (Falcon, reference 352350). Then, 100-μl samples of the obtained cell fractions were used for flow cytometry studies.

Histopathologic and immunohistochemical analyses were performed using formalin-fixed, paraffin-embedded mouse BM and tumor tissue samples. Slides were stained with hematoxylin and eosin or immunostained with mAbs against B220 and CD138, followed by secondary antibodies linked to horseradish peroxidase.

Serum electrophoresis and Ig isotypes

Blood samples were extracted from mice at the time of euthanasia, collected in Microvette 55 Z-Gel tubes (Sarstedt, reference 20.1344), and centrifuged at 10,000*g* for 5 min at room temperature. After centrifugation and serum recovery, electrophoresis was performed in Hydragel Protein(E) agarose gel (Selbia) for measurement of Ig fractions. Ig isotype in serum samples from mice was determined using magnetic beads with the MILLIPLEX Map Kit (Merck). Briefly, serum samples were added to a 96-well plate together with anti-mouse IgA, IgG1, IgG2a, IgG2b, IgG3, and IgM beads. After incubation and subsequent washout, the plate was read in a Luminex MAGPIX instrument system (Thermo Fisher Scientific).

Statistical analysis

Mann-Whitney, Kruskal-Wallis, analysis of variance (ANOVA), Wilcoxon, and chi square tests were used to determine if differences between groups were statistically significant, as specified in Results and respective figures. All significance tests were two-tailed, and a *P* value of 0.05 was used as the threshold for statistical significance. TTP was estimated using Kaplan-Meier methodology and compared between groups using a two-sided log-rank test. TTP was measured from the time of immunophenotypic studies being performed until the date of determination of LPL/WM disease relapse/progression; patients without progressive disease at the time of last follow-up were censored at this time point. Statistical analyses were

performed with Stata (version 15.0; StataCorp LP, TX) and SPSS (version 20.0; IBM, Chicago, IL).

SUPPLEMENTARY MATERIALS

Supplementary material for this article is available at https://science.org/doi/10.1126/sciadv.abl4644

View/request a protocol for this paper from *Bio-protocol*.

REFERENCES AND NOTES

1. N. Wijewardhane, L. Dressler, F. D. Ciccarelli, Normal somatic mutations in cancer transformation. *Cancer Cell* **39**, 125–129 (2020).
2. K. Yoshida, K. H. C. Gowers, H. Lee-Six, D. P. Chandrasekharan, T. Coorens, E. F. Maughan, K. Beal, A. Menzies, F. R. Millar, E. Anderson, S. E. Clarke, A. Pennycuick, R. M. Thakrar, C. R. Butler, N. Kakiuchi, T. Hirano, R. E. Hynds, M. R. Stratton, I. Martincorena, S. M. Janes, P. J. Campbell, Tobacco smoking and somatic mutations in human bronchial epithelium. *Nature* **578**, 266–272 (2020).
3. Y. Li, Y. Jiang, J. Paxman, R. O'Laughlin, S. Klepin, Y. Zhu, L. Pillus, L. S. Tsimring, J. Hasty, N. Hao, A programmable fate decision landscape underlies single-cell aging in yeast. *Science* **369**, 325–329 (2020).
4. I. Martincorena, J. C. Fowler, A. Wabik, A. R. J. Lawson, F. Abascal, M. W. J. Hall, A. Cagan, K. Murai, K. Mahbubani, M. R. Stratton, R. C. Fitzgerald, P. A. Handford, P. J. Campbell, K. Saeb-Parsy, P. H. Jones, Somatic mutant clones colonize the human esophagus with age. *Science* **362**, 911–917 (2018).
5. A. R. J. Lawson, F. Abascal, T. H. H. Coorens, Y. Hooks, L. O'Neill, C. Latimer, K. Raine, M. A. Sanders, A. Y. Warren, K. T. A. Mahbubani, B. Bareham, T. M. Butler, L. M. R. Harvey, A. Cagan, A. Menzies, L. Moore, A. J. Colquhoun, W. Turner, B. Thomas, V. Gnanapragasam, N. Williams, D. M. Rassl, H. Vöhringer, S. Zumalave, J. Nangalia, J. M. C. Tubío, M. Gerstung, K. Saeb-Parsy, M. R. Stratton, P. J. Campbell, T. J. Mitchell, I. Martincorena, Extensive heterogeneity in somatic mutation and selection in the human bladder. *Science* **370**, 75–82 (2020).
6. H. Lee-Six, S. Olafsson, P. Ellis, R. J. Osborne, M. A. Sanders, L. Moore, N. Georgakopoulos, F. Torrente, A. Noorani, M. Goddard, P. Robinson, T. H. H. Coorens, L. O'Neill, C. Alder, J. Wang, R. C. Fitzgerald, M. Zilbauer, N. Coleman, K. Saeb-Parsy, I. Martincorena, P. J. Campbell, M. R. Stratton, The landscape of somatic mutation in normal colorectal epithelial cells. *Nature* **574**, 532–537 (2019).
7. S. Olafsson, R. E. M. Intyre, T. Coorens, T. Butler, H. Jung, P. S. Robinson, H. Lee-Six, M. A. Sanders, K. Arestang, C. Dawson, M. Tripathi, K. Strongili, Y. Hooks, M. R. Stratton, M. Parkes, I. Martincorena, T. Raine, P. J. Campbell, C. A. Anderson, Somatic evolution in non-neoplastic IBD-affected colon. *Cell* **182**, 672–684.e11 (2020).
8. L. Moore, D. Leongamornlert, T. H. H. Coorens, M. A. Sanders, P. Ellis, S. C. Dentro, K. J. Dawson, T. Butler, R. Rahbari, T. J. Mitchell, F. Maura, J. Nangalia, P. S. Tarpey, S. F. Brunner, H. Lee-Six, Y. Hooks, S. Moody, K. T. Mahbubani, M. Jimenez-Linan, J. J. Brosens, C. A. Iacobuzio-Donahue, I. Martincorena, K. Saeb-Parsy, P. J. Campbell, M. R. Stratton, The mutational landscape of normal human endometrial epithelium. *Nature* **580**, 640–646 (2020).
9. M. S. Anglesio, N. Papadopoulos, A. Ayhan, T. M. Nazeran, M. Noë, H. M. Horlings, A. Lum, S. Jones, J. Senz, T. Seckin, J. Ho, R.-C. Wu, V. Lac, H. Ogawa, B. Tessier-Cloutier, R. Alhassan, A. Wang, Y. Wang, J. D. Cohen, F. Wong, A. Hasanovic, N. Orr, M. Zhang, M. Popoli, W. McMahon, L. D. Wood, A. Mattox, C. Allaire, J. Segars, C. Williams, C. Tomasetti, N. Boyd, K. W. Kinzler, C. B. Gilks, L. Diaz, T.-L. Wang, B. Vogelstein, P. J. Yong, D. G. Huntsman, I.-M. Shih, Cancer-associated mutations in endometriosis without cancer. *N. Engl. J. Med.* **376**, 1835–1848 (2017).
10. M. Zhu, T. Lu, Y. Jia, X. Luo, P. Gopal, L. Li, M. Odewole, V. Renteria, A. G. Singal, Y. Jang, K. Ge, S. C. Wang, M. Sorouri, J. R. Parekh, M. P. MacConmara, A. C. Yopp, T. Wang, H. Zhu, Somatic mutations increase hepatic clonal fitness and regeneration in chronic liver disease. *Cell* **177**, 608–621.e12 (2019).
11. S. F. Brunner, N. D. Roberts, L. A. Wylie, L. Moore, S. J. Aitken, S. E. Davies, M. A. Sanders, P. Ellis, C. Alder, Y. Hooks, F. Abascal, M. R. Stratton, I. Martincorena, M. Hoare, P. J. Campbell, Somatic mutations and clonal dynamics in healthy and cirrhotic human liver. *Nature* **574**, 538–542 (2019).
12. A. Yokoyama, N. Kakiuchi, T. Yoshizato, Y. Nannya, H. Suzuki, Y. Takeuchi, Y. Shiozawa, Y. Sato, K. Aoki, S. K. Kim, Y. Fujii, K. Yoshida, K. Kataoka, M. M. Nakagawa, Y. Inoue, T. Hirano, Y. Shiraishi, K. Chiba, H. Tanaka, M. Sanada, Y. Nishikawa, Y. Amanuma, S. Ohashi, I. Aoyama, T. Horimatsu, S. Miyamoto, S. Tsunoda, Y. Sakai, M. Narahara, J. B. Brown, Y. Sato, G. Sawada, K. Mimori, S. Minamiguchi, H. Haga, H. Seno, S. Miyano, H. Makishima, M. Muto, S. Ogawa, Age-related remodelling of oesophageal epithelia by mutated cancer drivers. *Nature* **565**, 312–317 (2019).
13. B. Colom, M. P. Alcolea, G. Piedrafita, M. W. J. Hall, A. Wabik, S. C. Dentro, J. C. Fowler, A. Herms, C. King, S. H. Ong, R. K. Sood, M. Gerstung, I. Martincorena, B. A. Hall, P. H. Jones, Spatial competition shapes the dynamic mutational landscape of normal esophageal epithelium. *Nat. Genet.* **52**, 604–614 (2020).
14. I. Martincorena, A. Roshan, M. Gerstung, P. Ellis, P. Van Loo, S. McLaren, D. C. Wedge, A. Fullam, L. B. Alexandrov, J. M. Tubio, L. Stebbings, A. Menzies, S. Widaa, M. R. Stratton, P. H. Jones, P. J. Campbell, High burden and pervasive positive selection of somatic mutations in normal human skin. *Science (80-.)*. **348**, 880–886 (2015).
15. G. A. Challen, M. A. Goodell, Clonal hematopoiesis: Mechanisms driving dominance of stem cell clones. *Blood* **136**, 1590–1598 (2020).
16. J. T. Warren, D. C. Link, Clonal hematopoiesis and risk for hematologic malignancy. *Blood* **136**, 1599–1605 (2020).
17. C. J. Watson, A. L. Papula, G. Y. P. Poon, W. H. Wong, A. L. Young, T. E. Druley, D. S. Fisher, J. R. Blundell, The evolutionary dynamics and fitness landscape of clonal hematopoiesis. *Science (80-.)*. **367**, 1449–1454 (2020).
18. L. M. Slot, T. A. M. Wormhoudt, M. J. Kwakkenbos, K. Wagner, A. Ballering, A. Jongejan, A. C. M. van Kampen, J. E. J. Guikema, R. J. Bende, C. J. M. van Noesel, De novo gene mutations in normal human memory B cells. *Leukemia* **33**, 1219–1230 (2019).
19. L. Zhang, X. Dong, M. Lee, A. Y. Maslov, T. Wang, J. Vijg, Single-cell whole-genome sequencing reveals the functional landscape of somatic mutations in B lymphocytes across the human lifespan. *Proc. Natl. Acad. Sci. U.S.A.* **116**, 9014–9019 (2019).
20. M. Singh, G. Al-Eryani, S. Carswell, J. M. Ferguson, J. Blackburn, K. Barton, D. Roden, F. Luciani, T. Giang Phan, S. Junankar, K. Jackson, C. C. Goodnow, M. A. Smith, A. Swarbrick, High-throughput targeted long-read single cell sequencing reveals the clonal and transcriptional landscape of lymphocytes. *Nat. Commun.* **10**, 3120 (2019).
21. Y. Kikushige, F. Ishikawa, T. Miyamoto, T. Shima, S. Urata, G. Yoshimoto, Y. Mori, T. Iino, T. Yamauchi, T. Eto, H. Niiro, H. Iwasaki, K. Takenaka, K. Akashi, Self-renewing hematopoietic stem cell is the primary target in pathogenesis of human chronic lymphocytic leukemia. *Cancer Cell* **20**, 246–259 (2011).
22. S. S. Chung, E. Kim, J. H. Park, Y. R. Chung, P. Lito, J. Teruya-Feldstein, W. Hu, W. Beguelin, S. Monette, C. Duy, R. Rampal, L. Telis, M. Patel, M. K. Kim, K. Huberman, N. Bouvier, M. F. Berger, A. M. Melnick, N. Rosen, M. S. Tallman, C. Y. Park, O. Abdel-Wahab, Hematopoietic stem cell origin of BRAFV600E mutations in hairy cell leukemia. *Sci. Transl. Med.* **6**, 238ra71 (2014).
23. A. Agathangelidis, V. Ljungström, L. Scarfò, C. Fazi, M. Gounari, T. Pandzic, L. A. Sutton, K. Stamatopoulos, G. Tonon, R. Rosenquist, P. Ghia, Highly similar genomic landscapes in monoclonal b-cell lymphocytosis and ultra-stable chronic lymphocytic leukemia with low frequency of driver mutations. *Haematologica* **103**, 865–873 (2018).
24. F. Damm, E. Mylonas, A. Cosson, K. Yoshida, V. Della Valle, E. Mouly, M. Diop, L. Scourzic, Y. Shiraishi, K. Chiba, H. Tanaka, S. Miyano, Y. Kikushige, F. Davi, J. Lambert, D. Gautheret, H. Merle-Béral, L. Sutton, P. Dessen, E. Solary, K. Akashi, W. Vainchenker, T. Mercher, N. Droin, S. Ogawa, F. Nguyen-Khac, O. A. Bernard, Acquired initiating mutations in early hematopoietic cells of CLL patients. *Cancer Discov.* **4**, 1088–1101 (2014).
25. J. D. Phelan, R. M. Young, D. E. Webster, S. Roulland, G. W. Wright, M. Kasbekar, A. L. Shaffer, M. Ceribelli, J. Q. Wang, R. Schmitz, M. Nakagawa, E. Bachy, D. W. Huang, Y. Ji, L. Chen, Y. Yang, H. Zhao, X. Yu, W. Xu, M. M. Palisoc, R. R. Valadez, T. Davies-Hill, W. H. Wilson, W. C. Chan, E. S. Jaffe, R. D. Gascoyne, E. Campo, A. Rosenwald, G. Ott, J. Delabie, L. M. Rimsza, F. J. Rodriguez, F. Estephan, M. Holdhoff, M. J. Kruhlak, S. M. Hewitt, C. J. Thomas, S. Pittaluga, T. Oellerich, L. M. Staudt, A multiprotein supercomplex controlling oncogenic signalling in lymphoma. *Nature* **560**, 387–391 (2018).
26. X. Yu, W. Li, Q. Deng, H. Liu, X. Wang, H. Hu, Y. Cao, Z. Y. Xu-Monette, L. Li, M. Zhang, Z. Lu, K. H. Young, Y. Li, MYD88 L265P elicits mutation-specific ubiquitination to drive NF-κB activation and lymphomagenesis. *Blood* **137**, 1615–1627 (2021).
27. S. P. Treon, L. Xu, M. L. Guerrera, C. Jimenez, Z. R. Hunter, X. Liu, M. Demos, J. Gustine, G. Chan, M. Munshi, N. Tsakmaklis, J. G. Chen, A. Kofides, R. Sklavenitis-Pistofidis, M. Bustoros, A. Keezer, K. Meid, C. J. Patterson, A. Sacco, A. Roccaro, A. R. Branagan, G. Yang, I. M. Ghobrial, J. J. Castillo, Genomic landscape of Waldenström macroglobulinemia and its impact on treatment strategies. *J. Clin. Oncol.* **38**, 1198–1208 (2020).
28. R. A. L. de Groen, A. M. R. Schrader, M. J. Kersten, S. T. Pals, J. S. P. Vermaat, MYD88 in the driver's seat of B-cell lymphomagenesis: From molecular mechanisms to clinical implications. *Haematologica* **104**, 2337–2348 (2019).
29. E. Kastritis, V. Leblond, M. A. Dimopoulos, E. Kimby, P. Staber, M. J. Kersten, A. Tedeschi, C. Buske; ESMO Guidelines Committee, Waldenström's macroglobulinaemia: ESMO Clinical Practice Guidelines for diagnosis, treatment and follow-up. *Ann. Oncol.* **29**, iv41–iv50 (2018).
30. L. Xu, Z. R. Hunter, G. Yang, Erratum: MYD88 L265P in Waldenström macroglobulinemia, immunoglobulin M monoclonal gammopathy, and other B-cell lymphoproliferative disorders using conventional and quantitative allele-specific polymerase chain reaction (Blood (2013) 121:11 (2051-2058)). *Blood* **121**, 5259 (2013).
31. C. Jiménez, E. Sebastián, M. C. Chillón, P. Giraldo, J. Mariano Hernández, F. Escalante, T. J. González-López, C. Aguilera, A. G. De Coca, I. Murillo, M. Alcoceba, A. Balanzategui, M. E. Sarasquete, R. Corral, L. A. Marín, B. Paiva, E. M. Ocio, N. C. Gutiérrez, M. González, J. F. San Miguel, R. García-Sanz, MYD88 L265P is a marker highly characteristic of, but not restricted to, Waldenström's macroglobulinemia. *Leukemia* **27**, 1722–1728 (2013).

32. R. A. Kyle, D. R. Larson, T. M. Therneau, A. Dispenzieri, S. Kumar, J. R. Cerhan, S. V. Rajkumar, Long-term follow-up of monoclonal gammopathy of undetermined significance. *N. Engl. J. Med.* **378**, 241–249 (2018).

33. B. Paiva, L. A. Corchete, M. B. Vidriales, R. García-Sanz, J. J. Perez, I. Aires-Mejia, M. L. Sanchez, P. Barcena, D. Alignani, C. Jimenez, M. E. Sarasquete, M. V. Mateos, E. M. Ocio, N. Puig, F. Escalante, J. Hernández, R. Cuello, A. G. De Coca, M. Sierra, M. C. Montes, T. J. González-López, J. Galende, A. Bárez, J. Alonso, E. Pardal, A. Orfao, N. C. Gutierrez, J. F. San Miguel, The cellular origin and malignant transformation of waldenström macroglobulinemia. *Blood* **125**, 2370–2380 (2015).

34. D. Drandi, E. Genuardi, I. Dogliotti, M. Ferrante, C. Jiménez, F. Guerrini, M. Lo Schirico, B. Mantoan, V. Muccio, G. Lia, G. M. Zaccaria, P. Omedè, R. Passera, L. Orsucci, G. Benevolo, F. Cavallo, S. Galimberti, R. G. Sanz, M. Boccadoro, M. Ladetto, S. Ferrero, Highly sensitive MYD88 l265p mutation detection by droplet digital polymerase chain reaction in waldenström macroglobulinemia. *Haematologica* **103**, 1029–1037 (2018).

35. E. Braggio, C. Philipsborn, A. Novak, L. Hodge, S. Ansell, R. Fonseca, Molecular pathogenesis of Waldenstrom's macroglobulinemia. *Haematologica* **97**, 1281–1290 (2012).

36. G. Knittel, P. Liedgens, D. Korovkina, J. M. Seeger, Y. Al-Baldawi, M. Al-Maarri, C. Fritz, K. Vlantis, S. Bezhanova, A. H. Scheel, O. O. Wolz, M. Reimann, P. Möller, C. López, M. Schlesner, P. Lohneis, A. N. R. Weber, L. Trümper; German International Cancer Genome Consortium Molecular Mechanisms in Malignant Lymphoma by Sequencing Project Consortium, L. M. Staudt, M. Ortmann, M. Pasparakis, R. Siebert, C. A. Schmitt, A. R. Klatt, F. T. Wunderlich, S. C. Schäfer, T. Persigehl, M. Montesinos-Rongen, M. Odenthal, R. Büttner, L. P. Frenzel, H. Kashkar, H. C. Reinhardt, B-cell-specific conditional expression of Myd88p.L252P leads to the development of diffuse large B-cell lymphoma in mice. *Blood* **127**, 2732–2741 (2016).

37. T. Sewastianik, M. L. Guerrera, K. Adler, P. S. Dennis, K. Wright, V. Shanmugam, Y. Huang, H. Tanton, M. Jiang, A. Kofides, M. G. Demos, A. Dalgarno, N. A. Patel, A. Nag, G. S. Pinkus, G. Yang, Z. R. Hunter, P. Jarolim, N. C. Munshi, S. P. Treon, R. D. Carrasco, Human MYD88L265P is insufficient by itself to drive neoplastic transformation in mature mouse B cells. *Blood Adv.* **3**, 3360–3374 (2019).

38. Y. Cao, G. Yang, Z. R. Hunter, X. Liu, L. Xu, J. Chen, N. Tsakmaklis, E. Hatjiharissi, S. Kanan, M. S. Davids, J. J. Castillo, S. P. Treon, The BCL2 antagonist ABT-199 triggers apoptosis, and augments ibrutinib and idelalisib mediated cytotoxicity in CXCR4 wild-type and CXCR4 WHIM mutated waldenstrom macroglobulinaemia cells. *Br. J. Haematol.* **170**, 134–138 (2015).

39. A. Paulus, S. Akhtar, H. Yousaf, A. Manna, S. M. Paulus, Y. Bashir, T. R. Caulfield, M. Kuranz-Blake, K. Chitta, X. Wang, Y. Asmann, R. Hudec, W. Springer, S. Ailawadhi, A. Chanan-Khan, Waldenstrom macroglobulinemia cells devoid of BTK C481S or CXCR4 WHIM-like mutations acquire resistance to ibrutinib through upregulation of Bcl-2 and AKT resulting in vulnerability towards venetoclax or MK2206 treatment. *Blood Cancer J.* **7**, e565 (2017).

40. S. C. Dentro, I. Leshchiner, K. Haase, M. Tarabichi, J. Wintersinger, A. G. Deshwar, K. Yu, Y. Rubanova, G. Macintyre, J. Demeulemeester, I. Vázquez-García, K. Kleinheinz, D. G. Livitz, S. Malikic, N. Donmez, S. Sengupta, P. Anur, C. Jolly, M. Cmero, D. Rosebrock, S. E. Schumacher, Y. Fan, M. Fittall, R. M. Drews, X. Yao, T. B. K. Watkins, J. Lee, M. Schlesner, H. Zhu, D. J. Adams, N. McGranahan, C. Swanton, G. Getz, P. C. Boutros, M. Imielinski, R. Beroukhim, S. C. Sahinalp, Y. Ji, M. Peifer, I. Martincorena, F. Markowetz, V. Mustonen, K. Yuan, M. Gerstung, P. T. Spellman, W. Wang, Q. D. Morris, D. C. Wedge, P. Van Loo, S. C. Dentro, I. Leshchiner, M. Gerstung, C. Jolly, K. Haase, M. Tarabichi, J. Wintersinger, A. G. Deshwar, K. Yu, S. Gonzalez, Y. Rubanova, G. Macintyre, J. Demeulemeester, D. J. Adams, P. Anur, R. Beroukhim, P. C. Boutros, D. D. Bowtell, P. J. Campbell, S. Cao, E. L. Christie, M. Cmero, Y. Cun, K. J. Dawson, N. Donmez, R. M. Drews, R. Eils, Y. Fan, M. Fittall, D. W. Garsed, G. Getz, G. Ha, M. Imielinski, L. Jerman, Y. Ji, K. Kleinheinz, J. Lee, H. Lee-Six, D. G. Livitz, S. Malikic, F. Markowetz, I. Martincorena, T. J. Mitchell, V. Mustonen, L. Oesper, M. Peifer, M. Peto, B. J. Raphael, D. Rosebrock, S. C. Sahinalp, A. Salcedo, M. Schlesner, S. E. Schumacher, S. Sengupta, R. Shi, S. J. Shin, L. D. Stein, O. Spiro, I. Vázquez-García, S. Vembu, D. A. Wheeler, T.-P. Yang, X. Yao, K. Yuan, H. Zhu, W. Wang, Q. D. Morris, P. T. Spellman, D. C. Wedge, P. Van Loo; PCAWG Evolution and Heterogeneity Working Group and the PCAWG Consortium, Characterizing genetic intra-tumor heterogeneity across 2,658 human cancer genomes. *Cell* **184**, 2239–2254.e39 (2021).

41. L. B. Alexandrov, J. Kim, N. J. Haradhvala, M. N. Huang, A. W. T. Ng, Y. Wu, A. Boot, K. R. Covington, D. A. Gordenin, E. N. Bergstrom, S. M. A. Islam, N. Lopez-Bigas, L. J. Klimczak, J. R. McPherson, S. Morganella, R. Sabarinathan, D. A. Wheeler, V. Mustonen, L. B. Alexandrov, E. N. Bergstrom, A. Boot, P. Boutros, K. Chan, K. R. Covington, A. Fujimoto, G. Getz, D. A. Gordenin, N. J. Haradhvala, M. N. Huang, S. M. A. Islam, M. Kazanov, J. Kim, L. J. Klimczak, N. Lopez-Bigas, M. Lawrence, I. Martincorena, J. R. McPherson, S. Morganella, V. Mustonen, H. Nakagawa, A. W. T. Ng, P. Polak, S. Prokopec, S. A. Roberts, S. G. Rozen, R. Sabarinathan, N. Saini, T. Shibata, Y. Shiraishi, M. R. Stratton, B. T. Teh, I. Vázquez-García, D. A. Wheeler, Y. Wu, F. Yousif, W. Yu, G. Getz,

42. S. G. Rozen, M. R. Stratton, The repertoire of mutational signatures in human cancer. *Nature* **578**, 94–101 (2020).

43. A. M. Roccaro, A. Sacco, C. Jimenez, P. Maiso, M. Moschetta, Y. Mishima, Y. Aljawai, I. Sahin, M. Kuhne, P. Cardarelli, L. Cohen, J. F. San Miguel, R. Garcia-Sanz, I. M. Ghobrial, C1013G/CXCR4 acts as a driver mutation of tumor progression and modulator of drug resistance in lymphoplasmacytic lymphoma. *Blood* **123**, 4120–4131 (2014).

44. V. N. Ngo, R. M. Young, R. Schmitz, S. Jhavar, W. Xiao, K. H. Lim, H. Kohlhammer, W. Xu, Y. Yang, H. Zhao, A. L. Shaffer, P. Romesser, G. Wright, J. Powell, A. Rosenwald, H. K. Muller-Hermelink, G. Ott, R. D. Gascoyne, J. M. Connors, L. M. Rimsza, E. Campo, E. S. Jaffe, J. Delabie, E. B. Smeland, R. I. Fisher, R. M. Braziel, R. R. Tubbs, J. R. Cook, D. D. Weisenburger, W. C. Chan, L. M. Staudt, Oncogenically active MYD88 mutations in human lymphoma. *Nature* **470**, 115–119 (2011).

45. G. Yang, Y. Zhou, X. Liu, L. Xu, Y. Cao, R. J. Manning, C. J. Patterson, S. J. Buhrlage, N. Gray, Y. T. Tai, K. C. Anderson, Z. R. Hunter, S. P. Treon, A mutation in MYD88 (L265P) supports the survival of lymphoplasmacytic cells by activation of Bruton tyrosine kinase in Waldenström macroglobulinemia. *Blood* **122**, 1222–1232 (2013).

46. T. Kalina, J. Flores-Montero, V. H. J. Van Der Velden, M. Martin-Ayuso, S. Böttcher, M. Ritgen, J. Almeida, L. Lhermitte, V. Asnafi, A. Mendonça, R. De Tute, M. Cullen, L. Sedek, M. B. Vidriales, J. J. Pérez, J. G. Te Marvelde, E. Mejstrikova, O. Hrusak, T. Szczepaski, J. J. M. Van Dongen, A. Orfao; EuroFlow Consortium (EU-FP6, LSHB-CT-2006-018708), EuroFlow standardization of flow cytometer instrument settings and immunophenotyping protocols. *Leukemia* **26**, 1986–2010 (2012).

47. M. Jongen-Lavrencic, T. Grob, D. Hanekamp, F. G. Kavelaars, A. al Hinai, A. Zeilemaker, C. A. J. Erpelinck-Verschueren, P. L. Gradowska, R. Meijer, J. Cloos, B. J. Biemond, C. Graux, M. van Marwijk Kooy, M. G. Manz, T. Pabst, J. R. Passweg, V. Havelange, G. J. Ossenkoppele, M. A. Sanders, G. J. Schuurhuis, B. Löwenberg, P. J. M. Valk, Molecular minimal residual disease in acute myeloid leukemia. *N. Engl. J. Med.* **378**, 1189–1199 (2018).

48. C. Jiménez, G. G. Chan, L. Xu, N. Tsakmaklis, A. Kofides, M. G. Demos, J. Chen, X. Liu, M. Munshi, G. Yang, J. J. Castillo, A. Wiestner, R. García-Sanz, S. P. Treon, Z. R. Hunter, Genomic evolution of ibrutinib-resistant clones in Waldenström macroglobulinaemia. *Br. J. Haematol.* **189**, 1165–1170 (2020).

49. R. García-Sanz, I. Dogliotti, G. M. Zaccaria, E. M. Ocio, A. Rubio, I. Murillo, F. Escalante, C. Aguilera, A. García-Mateo, A. G. de Coca, R. Hernández, J. Dávila, N. Puig, M. García-Álvarez, M. del Carmen Chillón, M. Alcoceba, A. Medina, V. G. de la Calle, M. E. Sarasquete, M. González, N. C. Gutiérrez, C. Jiménez, 6q deletion in Waldenström macroglobulinaemia negatively affects time to transformation and survival. *Br. J. Haematol.* **192**, 843–852 (2021).

49. A. A. Alizadeh, R. Majeti, Surprise! HSC are aberrant in chronic lymphocytic leukemia. *Cancer Cell* **20**, 135–136 (2011).

50. T. Reya, S. J. Morrison, M. F. Clarke, I. L. Weissman, Stem cells, cancer, and cancer stem cells. *Nature* **414**, 105–111 (2001).

51. R. Bjerkvig, B. B. Tysnes, K. S. Aboody, J. Najbauer, A. J. A. Terzis, The origin of the cancer stem cell: Current controversies and new insights. *Nat. Rev. Cancer* **5**, 899–904 (2005).

52. K. Schmidt, U. Sack, R. Graf, W. Winkler, O. Popp, P. Mertins, T. Sommermann, C. Kocks, K. Rajewsky, B-cell-specific Myd88 L252P expression causes a premalignant gammopathy resembling IgM MGUS. *Front. Immunol.* **11**, 602868 (2020).

53. C. Ouk, L. Roland, N. Gachard, S. Poulain, C. Oblet, D. Rizzo, A. Saintamand, Q. Lemasson, M. Carrion, M. Thomas, K. Balabanian, M. Espéli, M. Parrens, I. Soubeyran, M. Boulin, N. Faumont, J. Feuillard, C. Vincent-Fabert, Continuous MYD88 activation is associated with expansion and then transformation of IgM differentiating plasma cells. *Front. Immunol.* **12**, 641692 (2021).

54. Z. R. Hunter, L. Xu, G. Yang, Y. Zhou, X. Liu, Y. Cao, R. J. Manning, C. Tripsas, C. J. Patterson, P. Sheehy, S. P. Treon, The genomic landscape of Waldenström macroglobulinemia is characterized by highly recurring MYD88 and WHIM-like CXCR4 mutations, and small somatic deletions associated with B-cell lymphomagenesis. *Blood* **123**, 1637–1646 (2014).

55. M. L. Guerrera, N. Tsakmaklis, L. Xu, G. Yang, M. Demos, A. Kofides, G. G. Chan, R. J. Manning, X. Liu, J. G. Chen, M. Munshi, C. J. Patterson, J. J. Castillo, T. Dubeau, J. Gustine, R. D. Carrasco, L. Arcaini, M. Varettoni, M. Cazzola, S. P. Treon, Z. R. Hunter, MYD88 mutated and wild-type Waldenström's macroglobulinemia: Characterization of chromosome 6q gene losses and their mutual exclusivity with mutations in CXCR4. *Haematologica* **103**, e408–e411 (2018).

56. T. Jo, M. Nishikori, Y. Kogure, H. Arima, K. Sasaki, Y. Sasaki, T. Nakagawa, F. Iwai, S. Momose, A. Shiraishi, H. Kiyonari, T. Onuki, K. Shin-Ya, M. Yoshida, K. Kataoka, S. Ogawa, K. Iwai, A. Takaori-Kondo, LUBAC accelerates B-cell lymphomagenesis by conferring resistance to genotoxic stress on B cells. *Blood* **136**, 684–697 (2020).

57. B. Paiva, M. C. Montes, R. García-Sanz, E. M. Ocio, J. Alonso, N. D. L. Heras, F. Escalante, R. Cuello, A. G. De Coca, J. Galende, J. Hernández, M. Sierra, A. Martin, E. Pardal, A. Bárez, J. Alonso, L. Suarez, T. J. González-López, J. J. Perez, A. Orfao, M. B. Vidríales, J. F. S. Miguel,

Multiparameter flow cytometry for the identification of the Waldenström's clone in IgM-MGUS and Waldenström's macroglobulinemia: New criteria for differential diagnosis and risk stratification. *Leukemia* **28**, 166–173 (2014).

58. R. García-Sanz, E. M. Ocio, A. Caballero, R. J. P. Magalhães, J. Alonso, L. López-Anglada, T. Villaescusa, N. Puig, J. M. Hernández, J. Fernández-Calvo, A. Aguilar, A. Martín, R. López, B. Paiva, A. Orfao, B. Vidriales, J. F. San-Miguel, D. del Carpio, Post-treatment bone marrow residual disease > 5% by flow cytometry is highly predictive of short progression-free and overall survival in patients with Waldenström's macroglobulinemia. *Clin. Lymphoma Myeloma Leuk.* **11**, 168–171 (2011).

59. M. G. Demos, Z. R. Hunter, L. Xu, N. Tsakmaklis, A. Kofides, M. Munshi, X. Liu, M. L. Guerrera, C. R. Leventoff, T. P. White, C. A. Flynn, K. Meid, C. J. Patterson, G. Yang, A. R. Branagan, S. Sarosiek, J. J. Castillo, S. P. Treon, J. N. Gustine, Cell-free DNA analysis for detection of MYD88^{L265P} and CXCR4^{S338X} mutations in Waldenström macroglobulinemia. *Am. J. Hematol.* **96**, E250–E253 (2021).

60. J. N. Gustine, K. Meid, Z. R. Hunter, L. Xu, S. P. Treon, J. J. Castillo, *MYD88* mutations can be used to identify malignant pleural effusions in Waldenström macroglobulinaemia. *Br. J. Haematol.* **180**, 578–581 (2018).

61. I. S. Pagani, P. Dang, V. A. Saunders, J. Braley, A. Thieleke, S. Branford, T. P. Hughes, D. M. Ross, Clinical utility of genomic DNA Q-PCR for the monitoring of a patient with atypical e19a2 BCR-ABL1 transcripts in chronic myeloid leukemia. *Leuk. Lymphoma* **61**, 2527–2529 (2020).

62. P. Desai, N. Mencia-Trinchant, O. Savenkov, M. S. Simon, G. Cheang, S. Lee, M. Samuel, E. K. Ritchie, M. L. Guzman, K. V. Ballman, G. J. Roboz, D. C. Hassane, Somatic mutations precede acute myeloid leukemia years before diagnosis. *Nat. Med.* **24**, 1015–1023 (2018).

63. P. Theunissen, E. Mejstrikova, L. Sedek, A. J. Van Der Sluijs-Gelling, G. Gaipa, M. Bartels, E. S. da Costa, M. Kotrová, M. Novakova, E. Sonneveld, C. Buracchi, P. Bonaccorso, E. Oliveira, J. G. Te Marvelde, T. Szczepanski, L. Lhermitte, O. Hrusak, Q. Lecrevisse, G. E. Grigore, E. Fronková, J. Trka, M. Brüggemann, A. Orfao, J. J. M. Van Dongen, V. H. J. Van Der Velden; EuroFlow Consortium, Standardized flow cytometry for highly sensitive MRD measurements in B-cell acute lymphoblastic leukemia. *Blood* **129**, 347–357 (2017).

64. J. Flores-Montero, L. Sanoja-Flores, B. Paiva, N. Puig, O. García-Sánchez, S. Böttcher, V. H. J. van der Velden, J.-J. Pérez-Morán, M.-B. Vidriales, R. García-Sanz, C. Jimenez, M. González, J. Martínez-López, A. Corral-Mateos, G.-E. Grigore, R. Fluxá, R. Pontes, J. Caetano, L. Sedek, M.-C. Del Cañizo, J. Bladé, J.-J. Lahuerta, C. Aguilar, A. Bárez, A. García-Mateo, J. Labrador, P. Leoz, C. Aguilera-Sanz, J. San-Miguel, M.-V. Mateos, B. Durie, J. J. M. van Dongen, A. Orfao, Next generation flow for highly sensitive and standardized detection of minimal residual disease in multiple myeloma. *Leukemia* **31**, 2094–2103 (2017).

65. S. Mainardi, N. Mijimolle, S. Francoz, C. Vicente-Dueñas, I. Sánchez-García, M. Barbacid, Identification of cancer initiating cells in K-Ras driven lung adenocarcinoma. *Proc. Natl. Acad. Sci. U.S.A.* **111**, 255–260 (2014).

66. E. Hobeika, S. Thiemann, B. Storch, H. Jumaa, P. J. Nielsen, R. Pelanda, M. Reth, Testing gene function early in the B cell lineage in mb1-cre mice. *Proc. Natl. Acad. Sci. U.S.A.* **103**, 13789–13794 (2006).

67. S. Srinivas, T. Watanabe, C. S. Lin, C. M. William, Y. Tanabe, T. M. Jessell, F. Costantini, Cre reporter strains produced by targeted insertion of EYFP and ECFP into the ROSA26 locus. *BMC Dev. Biol.* **1**, 1–8 (2001).

68. S. Casola, G. Cattoretti, N. Uyttersprot, S. B. Koralov, J. Segal, Z. Hao, A. Waisman, A. Egert, D. Ghitza, K. Rajewsky, Tracking germinal center B cells expressing germ-line immunoglobulin 1 transcripts by conditional gene targeting. *Proc. Natl. Acad. Sci. U.S.A.* **103**, 7396–7401 (2006).

69. E. F. Robles, M. Mena-Varas, L. Barrio, S. V. Merino-Cortes, P. Balogh, M. Q. Du, T. Akasaka, A. Parker, S. Roa, C. Panizo, I. Martin-Guerrero, R. Siebert, V. Segura, X. Agirre, L. Macri-Pellizzeri, B. Aldaz, A. Vilas-Zornoza, S. Zhang, S. Moody, M. J. Calasanz, T. Tousseyn, C. Broccardo, P. Brousset, E. Campos-Sanchez, C. Cobaleda, I. Sanchez-Garcia, J. L. Fernandez-Luna, R. Garcia-Muñoz, E. Pena, B. Bellosillo, A. Salar, M. J. Baptista, J. M. Hernandez-Rivas, M. Gonzalez, M. J. Terol, J. Climent, A. Ferrandez, X. Sagaert, A. M. Melnick, F. Prosper, D. G. Oscier, Y. R. Carrasco, M. J. S. Dyer, J. A. Martinez-Climent, Homeobox NKX2-3 promotes marginal-zone lymphomagenesis by activating B-cell receptor signalling and shaping lymphocyte dynamics. *Nat. Commun.* **7**, 11889 (2016).

70. P. Marks, S. Garcia, A. M. Barrio, K. Belhocine, J. Bernate, R. Bharadwaj, K. Bjornson, C. Catalanotti, J. Delaney, A. Fehr, I. T. Fiddes, B. Galvin, H. Heaton, J. Herschleb, C. Hindson, E. Holt, C. B. Jabara, S. Jett, N. Keivanfar, S. Kyriazopoulou-Panagiotopoulou, M. Lek, B. Lin, A. Lowe, S. Mahamdallie, S. Maheshwari, T. Makarewicz, J. Marshall, F. Meschi, C. J. O'Keefe, H. Ordonez, P. Patel, A. Price, A. Royall, E. Ruark, S. Seal, M. Schnall-Levin, P. Shah, D. Stafford, S. Williams, I. Wu, A. W. Xu, N. Rahman, D. MacArthur, D. M. Church, Resolving the full spectrum of human genome variation using Linked-Reads. *Genome Res.* **29**, 635–645 (2019).

71. S. Chun, J. C. Fay, Identification of deleterious mutations within three human genomes. *Genome Res.* **19**, 1553–1561 (2009).

72. C. Dong, P. Wei, X. Jian, R. Gibbs, E. Boerwinkle, K. Wang, X. Liu, Comparison and integration of deleteriousness prediction methods for nonsynonymous SNVs in whole exome sequencing studies. *Hum. Mol. Genet.* **24**, 2125–2137 (2015).

73. H. A. Shihab, J. Gough, M. Mort, D. N. Cooper, I. N. M. Day, T. R. Gaunt, Ranking non-synonymous single nucleotide polymorphisms based on disease concepts. *Hum. Genomics* **8**, 11 (2014).

74. J. M. Schwarz, D. N. Cooper, M. Schuelke, D. Seelow, Mutationtaster2: Mutation prediction for the deep-sequencing age. *Nat. Methods* **11**, 361–362 (2014).

75. B. Reva, Y. Antipin, C. Sander, Predicting the functional impact of protein mutations: Application to cancer genomics. *Nucleic Acids Res.* **39**, e118 (2011).

76. Y. Choi, G. E. Sims, S. Murphy, J. R. Miller, A. P. Chan, Predicting the functional effect of amino acid substitutions and indels. *PLoS One.* **7**, e46688 (2012).

77. P. Kumar, S. Henikoff, P. C. Ng, Predicting the effects of coding non-synonymous variants on protein function using the SIFT algorithm. *Nat. Protoc.* **4**, 1073–1081 (2009).

78. E. V. Davydov, D. L. Goode, M. Sirota, G. M. Cooper, A. Sidow, S. Batzoglou, Identifying a high fraction of the human genome to be under selective constraint using GERP++. *PLoS Comput. Biol.* **6**, e1001025 (2010).

79. R. Valdés-Mas, S. Bea, D. A. Puente, C. López-Otín, X. S. Puente, Estimation of copy number alterations from exome sequencing data. *PLoS One.* **7**, e51422 (2012).

80. B. Gel, E. Serra, karyoploteR: An R/Bioconductor package to plot customizable genomes displaying arbitrary data. *Bioinformatics* **33**, 3088–3090 (2017).

81. Z. Gu, R. Eils, M. Schlesner, Complex heatmaps reveal patterns and correlations in multidimensional genomic data. *Bioinformatics* **32**, 2847–2849 (2016).

82. L. Zapata, H. Susak, O. Drechsel, M. R. Friedländer, X. Estivill, S. Ossowski, Signatures of positive selection reveal a universal role of chromatin modifiers as cancer driver genes. *Sci. Rep.* **7**, 13124 (2017).

83. L. Xu, Z. R. Hunter, G. Yang, Y. Zhou, Y. Cao, X. Liu, E. Morra, A. Trojani, A. Greco, L. Arcaini, M. Varettoni, J. R. Brown, Y. T. Tai, K. C. Anderson, N. C. Munshi, C. J. Patterson, R. J. Manning, C. K. Tripsas, N. I. Lindeman, S. P. Treon, MYD88 L265P in Waldenström macroglobulinemia, immunoglobulin M monoclonal gammopathy, and other B-cell lymphoproliferative disorders using conventional and quantitative allele-specific polymerase chain reaction. *Blood* **121**, 2051–2058 (2013).

84. C. Hafemeister, R. Satija, Normalization and variance stabilization of single-cell RNA-seq data using regularized negative binomial regression. *Genome Biol.* **20**, 296 (2019).